

Use Authorization

In presenting this thesis in partial fulfillment of the requirements for an advanced degree at Idaho State University, I agree that the Library shall make it freely available for inspection. I further state that permission to download and/or print my thesis for scholarly purposes may be granted by the Dean of the Graduate School, Dean of my academic division, or by the University Librarian. It is understood that any copying or publication of this thesis for financial gain shall not be allowed without my written permission.

Signature:

Date:

**Changes in Heat Shock Proteins and Mitochondrial Dynamics in Dorsal Root
Ganglion (DRG) Neurons Harboring Mitochondrial DNA Deletions:
Implications in Mitochondrial Dysfunction and Neurodegeneration**

By

Aishwarya Neti

**A Thesis Submitted in Partial Fulfillment of the Requirements for the M.S. in
Pharmaceutical Sciences at the Department of Biomedical and
Pharmaceutical Sciences, College of Pharmacy, Division of Health Sciences
Idaho State University.**

August 2014

© Aishwarya Neti

To the Graduate Faculty:

**The members of the committee appointed to examine the thesis of Aishwarya Neti find it
satisfactory and recommend that it be accepted.**

.....
James C. K. Lai, Ph.D,
Major Advisor

.....
James C. Bigelow, Ph.D,
Committee Member

.....
Solomon W. Leung, Ph.D,
Graduate Faculty Representative

This work is dedicated to my beloved parents and my brother

(Nataraj Sarma Neti, Nagamani Neti and Asrith Kumar Neti)

ACKNOWLEDGEMENTS

I offer my sincerest gratitude to my supervisor, Dr. James C.K. Lai, for his initial inputs in research and for supporting me throughout my research with his patience and knowledge while allowing me the room to work my own way.

I am deeply grateful to Dr. James C. Bigelow for his excellent guidance in Pharmaceutical Analysis and for providing me with the initial knowledge about research. I would also like to thank Dr. Alok Bhushan for being supportive while I pursue my M.S. degree and for helping me with developing my knowledge and background in drug discovery and oncology. A special thanks goes to Dr. Solomon W. Leung for sparing his valuable time to serve as a Graduate Faculty Representative in my committee.

I would love to thank my cheerful lab mates Anurag Kakkerla and Wenjuan Gao for their help throughout my research. I owe my deepest gratitude to Vinay Kumar for being extraordinarily tolerant and supportive and for helping me set up and trouble shoot experiments during the initial days of my research.

I would like to express my deepest appreciation to my other friends, Prabha Awale, Shabbir Lobo, Gaurav Sharma and Satya Tadinada for making my stay at Idaho State University wonderful.

I would also offer my thanks to the Graduate School, College of Pharmacy and Molecular Research Core Facility, Idaho State University for their financial and other support.

Finally, I would like to thank my parents and my brother for their support and encouragement and for standing by me throughout the good and bad times.

Table of Contents

List of figures	x
Abstract	xiv

Chapter 1

Introduction.....	2
Mitochondrial structure and function.....	2
Maintenance of mitochondrial DNA.....	5
Mitochondria and antioxidant systems.....	7
Mitochondrial dynamics and its importance.....	12
Heat shock proteins and their role in mitochondrial structure and function.....	13
Mitochondrial dysfunction in diseased states including neurodegeneration.....	14
Goals, scope and working hypothesis of my thesis research.....	19
References.....	20

Chapter 2

Differential effects of chronic mitochondrial DNA deletion on metabolism in Schwann cells and dorsal root ganglion neurons

Abstract.....	31
Introduction.....	32
Materials and Methods.....	34
Results.....	39
Discussion.....	46

Conclusions.....	47
Figures and Legends.....	49
Acknowledgements.....	49
References.....	66

Chapter 3

Mitochondrial DNA deletion in dorsal root ganglion neurons disrupts mitochondrial dynamics and induces changes in the expression of heat shock proteins

Abstract.....	71
Introduction.....	72
Materials and Methods.....	76
Results.....	80
Discussion.....	85
Conclusions.....	91
References.....	91
Figures and legends.....	97

Chapter 4

Conclusions and general discussion.....	110
Prospects for future studies.....	112
References.....	114

List of Figures

Chapter 1

- Figure 1. Figure depicting some of the functional components in the mitochondrial matrix.....3
- Figure 2. A schematic representation of the human mitochondrial genome.....6
- Figure 3. A flow chart depicting the responses during oxidative stress.....9

Chapter 2

- Figure 1. DRG neurons and Schwann cells and their respective ρ^0 cells viewed under light microscopy.....49
- Figure 2. Expression pattern of ND6 in DRG neurons treated with ethidium bromide over four weeks.....50
- Figure 3. Expression pattern of ND6 in Schwann cells treated with ethidium bromide over four weeks.....51
- Figure 4. Expression pattern of cytochrome c oxidase subunit 2 in DRG neurons treated with ethidium bromide over four weeks.....52
- Figure 5. Expression pattern of cytochrome c oxidase subunit 2 in Schwann cells treated with ethidium bromide over four weeks.....53

Figure 6. Expression pattern of Succinate Dehydrogenase in Schwann cells treated with ethidium bromide over four weeks.....	54
Figure 7. Expression pattern of Succinate dehydrogenase in DRG cells treated with ethidium bromide over four weeks.....	55
Figure 8. Effect of mtDNA deletion on mitochondrial mass in DRG neurons and Schwann cells.....	56
Figure 9. Citrate synthase activities in Schwann cells and DRG neurons and in their respective ρ^0 cells.....	57
Figure 10. Malate dehydrogenase activities in Schwann cells and DRG neurons and in their respective ρ^0 cells.....	58
Figure 11. Lactate dehydrogenase activities in Schwann cells and DRG neurons and in their respective ρ^0 cells.....	59
Figure 12. Hexokinase activities in Schwann cells and DRG neurons and in their respective ρ^0 cells.....	60
Figure 13. Expression pattern of MnSOD in Schwann cells and DRG neurons treated with ethidium bromide over four weeks.....	61
Figure 14. Effect of mtDNA deletion on expression of Mitofusin-1 (Mfn-1) in DRG neurons and Schwann cells.....	62
Figure 15. Effect of mtDNA deletion on expression of Mitofusin-2 (Mfn-2) in DRG neurons and Schwann cells.....	63

Figure 16. Effect of mtDNA deletion on mitochondrial dynamics in DRG neurons employing confocal microscopy.....	64
---	----

Chapter 3

Figure 1. Chronic exposure of DRG neurons to ethidium bromide (EB) induced time-related decreases in expression of NADH dehydrogenase subunit 6 (ND6).....	97
--	----

Figure 2. Chronic exposure of DRG neurons to ethidium bromide (EB) did not induce time-related decreases in expression of succinate dehydrogenase.....	98
--	----

Figure 3. Bright field light microscopic images of the control (i.e., not ethidium bromide (EB)-treated) and EB-treated DRG neurons.....	99
--	----

Figure 4. Chronic exposure of DRG neurons to ethidium bromide (EB) induced time-related decreases in expression of heat shock protein 70 (HSP70).....	100
---	-----

Figure 5. Chronic exposure of DRG neurons to ethidium bromide (EB) induced time-related decreases in expression of heat shock protein 90 (HSP90).....	101
---	-----

Figure 6. Chronic treatment with ethidium bromide (EB) induced decreased expression of optic atrophy factor-1 (OPA-1).....	102
--	-----

Figure 7. Chronic treatment with ethidium bromide (EB) induced increased expression of dynamic related protein-1 (DRP-1).....	103
---	-----

Figure 8. Chronic exposure of DRG neurons to ethidium bromide (EB) induced time-related decreases in expression of aconitase.....	104
---	-----

Figure 9. Bright field light microscopic images of control DRG neurons treated with only 50 μ M forskolin for 48 hours.....	105
---	-----

Figure 10. Chronic treatment with ethidium bromide (EB) induced decreased expression of synapsin-1.....	106
Figure 11. Production of reactive oxygen species (ROS) by control untreated DRG.....	107
Figure 12. Glutathione (GSH) content in control DRG neurons (i.e., not treated with EB) (DC) and DRG neurons chronically treated with ethidium bromide (EB).....	108

Abstract

Mutations and/or deletions in mtDNA, oxidative stress can induce mitochondrial dysfunction and neurodegeneration, but the mechanisms are poorly understood. To investigate the putative changes in the expressions of heat shock proteins, antioxidant proteins and mitochondrial fission and fusion proteins, we have developed cell models of mtDNA deletion employing dorsal root ganglion (DRG) neurons and Schwann cells — neural cell types in peripheral nervous system. We found chronic mtDNA depletion in DRG neurons and Schwann cells induced morphological changes, alterations in activities of key enzymes in oxidative metabolism, and enhanced their ROS production and impaired their antioxidant system. Additionally, mtDNA depletion disrupted mitochondrial dynamics and altered Hsp70 and Hsp90 expression in DRG neurons. Thus, our findings may assume pathophysiological importance in peripheral neuropathy in particular and neurodegeneration in general.

Chapter 1

Introduction

Chapter 1 contains a concise review of the literature relevant to the topics covered by the research presented herein, followed by the goals, scope and general hypothesis of the research. The work of this thesis was carried out in two phases. Phase 1 of this thesis was focused on characterizing the cell models, employing DRG neurons and Schwann cells. Phase 2 characterized some of the molecular changes occurring during deletions mitochondrial DNA and their implications in peripheral neuropathy and neurodegeneration.

Structure of mitochondria

Mitochondria, often described as the power house of the cell, play an important role in generation of energy in eukaryotic cells. The source of energy is mostly derived from the metabolism of carbohydrates, fatty acids, and amino acids. The produced and stored form of energy is ATP, which is produced by mitochondria mainly via oxidative phosphorylation. Although production of ATP appears to be the main role of mitochondria, they also play important roles in intermediary metabolism and synthesis of a variety of substances in the body (Krauss, 2001).

Mitochondria are double-membrane organelles consisting of the outer and inner membrane, separated by the inter-membrane space. (Fray and Manella, 2000). The inner membrane consists of numerous folds, called the cristae, which project into the matrix of the mitochondria. The two membranes represent distinct compartments in these organelle and are different in both structure and function (Mannella, 2006).

Both the outer and inner mitochondrial membranes composed of phospholipid bilayers, but the outer membrane has a special protein called porin, which can allow the passage of

molecules up to the size of 5000 Daltons into the matrix space (Martin et al., 2011). The outer membrane is highly permeable to smaller molecules and ions such as ATP and ADP. The inner membrane contains the various complexes of the electron transport chain (ETC) and ATP synthase complex: these complexes are interspersed among clusters of phospholipids and other structural proteins in the inner mitochondrial membrane. The inner mitochondrial membrane is only freely permeable to oxygen, carbon dioxide and water. The cristae of the inner membrane enhance the surface area of the inner mitochondrial membrane (Martin et al., 2011).

Within the confine of the mitochondrial matrix space (Fig. 1) are located enzymes of the tricarboxylic acid (TCA) cycle and enzymes of fatty acid and amino acid metabolism (Lai and Clark, 1989; Clark and Lai, 1989). Also within the matrix space are located the mitochondrial DNA (mtDNA) or the mitochondrial genome: their copy number varies between two and ten for mitochondria in mammalian cells (Mannella et al., 1997).

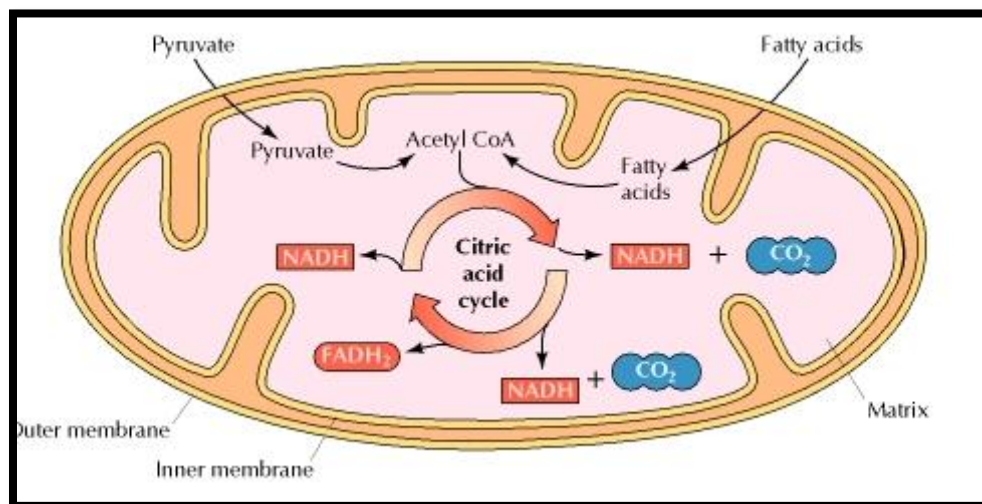


Figure 1: Figure depicting some of the functional components in the mitochondrial matrix (from Cooper and Sunderland, 2000).

Function of mitochondria

Even though the primary function of mitochondria is the production of energy in the form of ATP, they also play a vital role in cellular metabolism. The complex foods such as carbohydrates and fats are broken down into simpler intermediates and their final common end-product in intermediary metabolism is acetyl coenzyme A (CoA), which then enters the citric acid cycle, also known as tricarboxylic acid (TCA) cycle or Krebs' cycle (Lai and Clark, 1989; Clark and Lai, 1989; Lai, 1992). The major function of the TCA cycle is the generation of reducing equivalents, especially NADH, although NADPH and FADH_2 are also produced (Lai and Clark, 1989; Clark and Lai, 1989; Lai, 1992). These reducing equivalents (namely, NAD(P)H and FADH_2) are oxidized in the presence of oxygen via the electron transport chain (ETC) in the inner mitochondrial membrane and their re-oxidation is normally coupled to the generation of ATP through mitochondrial oxidative phosphorylation (OXPHOS) (Lai and Clark, 1989; Clark and Lai, 1989; Lai, 1992).

The ETC is composed of four multi-enzyme complexes (complex I-IV) and the ATP synthase (complex V), containing a total of some 80 or so polypeptides (Wallace, 2007). The complexes – complex I (NADH: ubiquinone oxidoreductase), complex III (ubiquinol cytochrome c reductase) and complex IV (cytochrome c oxidase) – are encoded by both nuclear and mitochondrial DNA. The complex II (succinate dehydrogenase) is encoded exclusively by the nuclear DNA. The rate of synthesis of ATP is highly regulated by the five ETC complexes (I-V). Hence the ETC has a vital role in regulating energy metabolism and damage of any of the complexes can lead to an impairment of ATP formation.

Mitochondria also play an important role in fatty acid metabolism and ketone body metabolism. The fatty acid β -oxidation is a series of reactions catalyzed by a group of enzymes that are located in the mitochondrial matrix and inner mitochondrial membrane (Cooper and Sunderland, 2000). Since the mitochondrial inner membrane is not permeable to long-chain fatty acids, a transport system called the carnitine transport of long-chain fatty acids has evolved for the transport of fatty acyl-CoA esters. There are two transporters called the carnitine palmitoyl transferase I and II (CPT I and CPT II) that are located on the mitochondrial outer membrane. They aid the transport of long-chain fatty acids (Cooper and Sunderland, 2000). The other metabolic pathways that take place in the mitochondria not directly linked to energy metabolism include heme synthesis and urea cycle (Cooper and Sunderland, 2000).

Maintenance of mitochondrial DNA

The genetic information in mammalian cells is stored in two locations, the nuclear DNA (nDNA) and mitochondrial DNA (mtDNA). Human mtDNA is a 16.6 kb circular double-stranded DNA that encodes 13 proteins, which are components of respiratory chain complexes (Fig. 2). The mitochondrial DNA encodes for 13 polypeptides in four of the five respiratory complexes, namely complex I, III, IV and V but not II: ND1-4, ND4L, ND5 and ND6 in the 45 polypeptides of complex I; cytochrome b (Cb) in the 11 subunits of complex III; CO (cytochrome oxidase) I, II and III in the 13 polypeptides of complex IV; and ATPase subunit 6 and ATPase subunit 8 of the ~16 subunits of complex V (Wallace, 2007). Because of this complexity in the cooperation between the genes of both mitochondrial and nuclear DNA in the biogenesis of the mitochondrial respiratory complexes (Wallace, 2007), any alterations in the mtDNA can lead to a number of potentially and/or actually life-threatening diseases.

A single mitochondrion harbors 2-10 molecules of mitochondrial DNA and under physiological conditions; the mitochondria form a dynamic network and assume various conformations (Shadel and Clayton, 1997; Shadel, 2008). The normal functioning of the cell depends upon the maintenance of mitochondrial DNA integrity and copy number. The maintenance of mitochondrial integrity and copy number is achieved through coordination between mtDNA replication, repair and degradation. However, the enzymes and other proteins required for mtDNA replication, transcription, and translation are nuclear DNA-encoded proteins and are imported into the mitochondrial matrix (Jeffery et al., 2006; Katsumi et al., 2014).

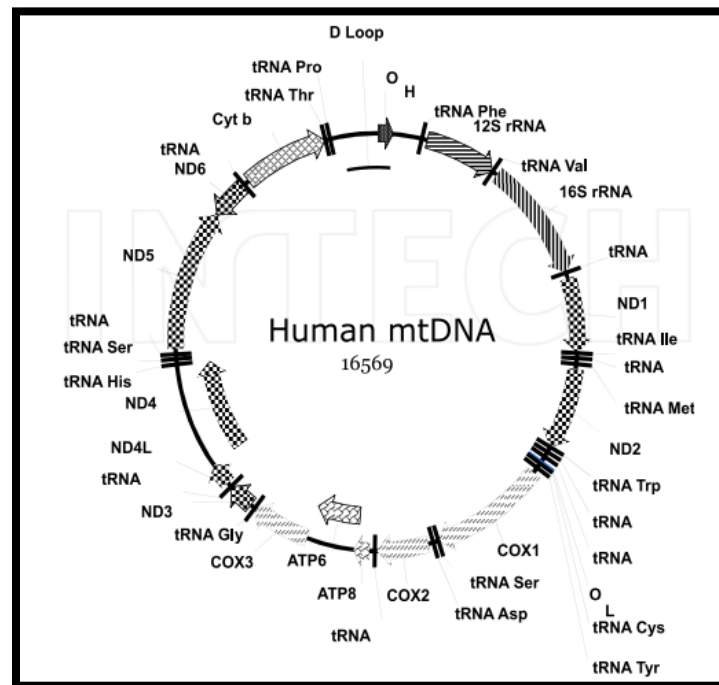


Figure 2. A schematic representation of the human mitochondrial genome (from Sholenko et al., 2002).

The mtDNA replication occurs in both dividing and non-dividing cells and takes place in all stages of cell cycle. The process of mtDNA replication is mediated by DNA polymerase

gamma (POLG) encoded by the POLG gene. Several other proteins, which play an important role in the replication of mitochondrial DNA, include DNA helicase twinkle, mitochondrial single strand binding protein (mtSSB), which facilitate unwinding, and mitochondrial RNA polymerase, which generates primers with the assistance of mitochondrial transcription factors A, B1 and B2 (TFAM, TFB1M, TFB2M, respectively) (Carlos et al., 1999).

The mtDNA is more susceptible to mutations than the nDNA as the mtDNA lacks the protection offered by the histone proteins and also because of the close proximity of the mtDNA to the production site of reactive oxygen species (ROS) (Gredilla, 2011). Historically, base excision repair (BER) pathway was thought of as the only pathway for the repair of mtDNA, but recently long patch BER and mismatch repair was reported in mammalian mitochondria (Gredilla, 2011). Moreover, mitochondria possess a unique mechanism for maintenance and repair of mtDNA through degradation of damaged molecules (Gredilla, 2011). Since there are perhaps hundreds of copies of mtDNA per cell, the “repair or die” constraint is not imposed on the cell and a substantial fraction of the mtDNA can be lost without repair as new strands of mtDNA are continuously being synthesized (Gredilla, 2011).

Mitochondria and antioxidant systems

Mitochondria have been described as the power house of the cell as they harness ATP by linking the energy releasing activities of the electron transport chain with the energy conserving process of oxidative phosphorylation. However, the electron-transfer reactions with their terminal acceptor being oxygen take place in the electron transport chain: some of these reactions can directly generate superoxide, which can dismutate to form hydrogen peroxide and can further react to form hydroxyl radical (Cadenas, 2000). These reactive oxygen species (ROS) are the most abundant free radicals in the cell and are the unavoidable products during normal

intracellular metabolism (Martin et al., 2007). Consequently, excessive ROS production can cause lipid peroxidation, DNA damage, protein oxidation and other oxidative damage in cells (Cadenas, 2000) (Fig. 3).

ROS induced DNA damage mainly includes strand break, cross linking, base hydroxylation and base excision (Cadenas, 2000). This consequently will result in mutagenesis and transformation of the mtDNA, especially if combined with an intracellular apoptotic pathway (Fig. 3).

The intracellular proteins are also the main targets of ROS. ROS can induce protein denaturation and enzyme inactivation as aromatic amino acids, cysteine and disulphide bonds are more susceptible to ROS (Chen et al., 2014).

Another class of free radicals includes reactive nitrogen species (RNS): they include nitric oxide and peroxynitrate (Irshad et al., 2002). Nitric oxide species usually attack intracellular thiol like glutathione and cysteine and metal-containing proteins (Irshad et al., 2002) (Fig. 3). Both deficiency and excess of RNS are involved in pathophysiological states like stroke of brain, ischemia, gastrointestinal dysfunction etc. (Irshad et al., 2002). Peroxynitrate also interacts with wide range of intracellular proteins and causes lipid peroxidation, thiol oxidation, tyrosine nitration, DNA strand break etc. and ultimately cell death (Irshad et al., 2002). When the concentration of both ROS and RNS exceeds the total antioxidant activity in the body, it results in a condition called oxidative stress (Irshad et al., 2002) (Fig. 3).

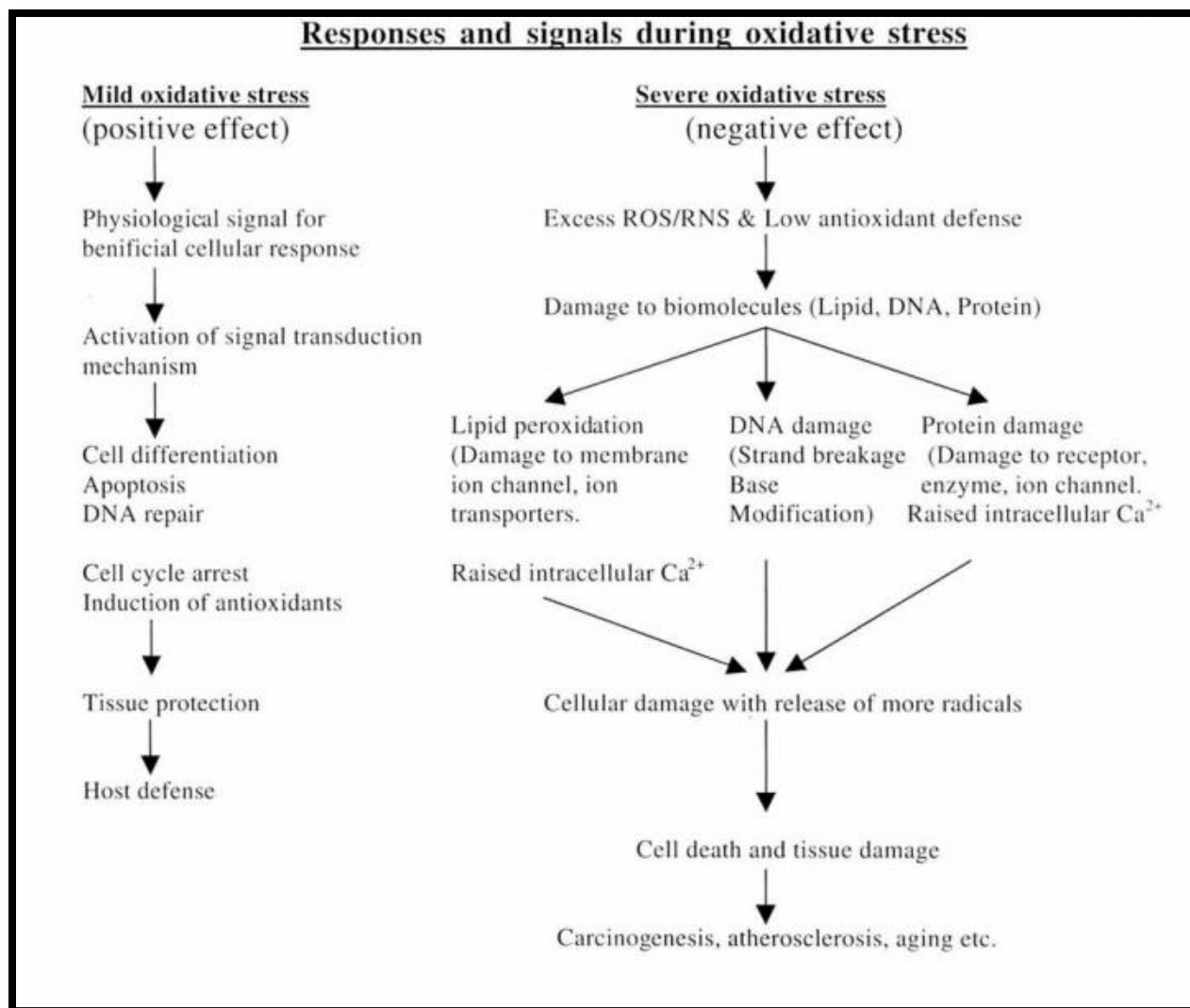


Figure 3. A flow chart depicting the responses during oxidative stress (from Irshad et al., 2002).

There are two main antioxidant systems in the body; enzymatic and non-enzymatic antioxidant systems that function to scavenge the free radicals in the body. The enzymatic antioxidant system, also called as the first line defense system includes superoxide dismutase (SOD), catalase (CAT), glutathione peroxidase (GPx) and glutathione reductase (GR). They usually catalyze sequentially the conversion of superoxide to hydrogen peroxide and hydrogen peroxide to water and oxygen (Lee et al., 2007; Isaac et al., 2007; Joachim et al, 2007). The non-

enzymatic antioxidant system or the second line defense system mostly comprises of vitamin C and vitamin E. They function by directly scavenging the free radicals by enhancing the activities of endogenous enzymatic antioxidants. Other non-enzymatic antioxidants include phenols, flavonoids, carotenoids naturally present in the foods (Simmi et al., 2004).

Mitochondrial dynamics

Mitochondrial dynamics play a vital role in many cell processes and are also crucial for ensuring mitochondrial quality control (Mannella, 2006). This in turn influences a number of mitochondrial properties like mitochondrial bioenergetics. Mitochondria undergo constant cycles of fission and fusion and impairment of the equilibrium between fission and fusion has been implicated in wide range of neurodegenerative diseases (Manella et al., 2000). The balance between the mitochondrial fission and fusion is important to maintain the morphology of the mitochondria. Mitochondrial fission is mainly important during differentiation of the cell, when tubular network of the mitochondria splits into small isolated organelles (Manella et al., 2006). On the other hand, mitochondrial fusion helps in maintaining the interconnected tubular network of the mitochondria (Bernard et al., 2009). Tubular network of the mitochondria facilitates effective oxygen transfer and in turn helps maintaining the membrane potential (Stefan et al., 2013).

Mitochondrial fusion

The first protein that was identified as a mediator of mitochondrial fusion was Fuzzy onions (FZO) in *Drosophila melanogaster*. It belongs to a class of large GTPases, called mitofusins. In mammals, two isoforms of mitofusins have been identified, mitofusin-1 and mitofusin-2 (Mfn-1 and Mfn-2). Another class of proteins that mediate the mitochondrial fusion

is dynamin related GTPase (Bernard et al., 2009). Mgm-1 isoform of the dynamin family has been identified in yeast and the mammalian isoform of Mgm-1 has been identified as optic atrophy factor-1 (OPA-1). In mammals, mitofusins along with OPA-1 are the core components of the fusion machinery (Michela et al., 2013). A membrane protein called Ugo-1 has been identified in yeast, which coordinates the fusion of the outer and inner membranes of the mitochondria. Mutations in the outer or inner membrane proteins severely affect the process of mitochondrial fusion, although the inner membrane and outer membrane fusion are independent (Zuchner et al., 2004).

Mitochondrial fusion: molecular mechanisms

Mfn1 and Mfn2 are required for mitochondrial fusion, and they are located in the mitochondrial outer membrane, where they can initiate the interaction of mitochondria with each other (Alexander et al., 2103). Mitofusins can form homotypic and heterotypic complexes during mitochondrial fusion and hence mitofusins are required on adjacent mitochondria during the membrane fusion event (Alexander et al., 2103). Homotypic Mfn1 complexes, homotypic Mfn2 complexes, and heterotypic Mfn1-Mfn2 complexes are competent for fusion (Alexander et al., 2103). A brief mechanistic summary of mitochondrial fusion can be described as follows (Alexander et al., 2103). The C-terminal region of Mfn1, containing the hydrophobic heptad repeat region HR2, can oligomerize with itself and with the analogous HR2 region from Mfn2. In this complex, such a structure would lead to close apposition of mitochondria. Therefore, the Mfn1 crystal structure likely represents a conformation of Mfn1 involved in the tethering of mitochondria. In vitro assays also support a role for Mfn1 in mitochondrial tethering. Mitochondrial fusion would require a conformational change that mediates closer apposition of

mitochondrial membranes and such a conformational change may occur by nucleotide-dependent changes in the GTPase domain (Alexander et al., 2013).

Mitochondrial fission

Mitochondrial fission is mediated by dynamin family of GTPase. The protein of the dynamin family, DNM-1 has been first identified in yeast and is one of the key components that mediate mitochondrial fission (Ferrier, 2001). Mammalian isoform of DNM-1 has been identified as DRP-1. The function of DRP-1 is dependent on two other dynamin class of proteins, mitochondrial fission-1 (fis-1) and mitochondrial division protein-1 (mdv-1). Fis-1 is present in the outer membrane of that provides an interface for the interaction between mdv-1 and DNM-1. The interaction between fis-1, mdv-1 and DNM-1 is important for mitochondrial division (Brigitte et al., 2001).

Mitochondrial fission: molecular mechanisms

The mitochondrial fission machinery consists of four proteins, namely fission-1 (fis1), which is present in the outer membrane while three other proteins are cytosolic proteins, which constitute dynamin-1 (Dnm 1) and two adapter proteins, mdv-1 and caf-4 (Marc et al., 2009). Extensive interconnected mitochondrial tubule like structures are present in the cells defective in outer membrane fission due to ongoing fusion, opposed by fission. Dnm1 is a dynamin-related protein containing an N-terminal GTPase domain, a middle domain, and a C-terminal GTPase effector domain. Cytosolic Dnm-1 is an important protein to mediate fission process and the mammalian homolog of Dnm-1 is DRP-1, which is also found to mediate fission process in other species such as worms and humans (Scott et al., 2010). Apart from Dnm-1, fis-1 and caf-4 are also important in mediating the fission process in mammals. The N-terminal of fis-1 exists in the

cytosol and forms a six-helix bundle containing tetratricopeptide repeated regions, which provide interaction interfaces for the other fission proteins in the cytosol. The mammalian homolog of fis-1 is termed hfis-1, which mediates the fission process in the cytosol (Emilie et al., 2006). While dnm-1 and fis-1 contain a separate domain, mdv-1 and caf-4 share the same domain and perform multiple functions in the cytosol. An N-terminal extension contains two helices that interact with Fis1, a coiled domain that mediates interactions and a C-terminal WD40 that binds with dnm-1. But the detailed structure and function of Mdv1 and Caf4 are still under investigation (Otera et al., 2011; Alexander et al., 2013).

Molecular chaperones and their role in mitochondrial structure and function

Heat shock proteins (HSPs) or molecular chaperones are essential for the survival of the cell as they are required for many cellular functions, like the house keeping tasks and stress protection. They interact with other proteins such as transferase of inner membrane and transferase of outer membrane (TIM and TOM) in the mitochondrial membrane for folding and unfolding of the proteins (Rassow et al., 1997). They also help in stabilizing the proteins by preventing irregular interactions, leading to denaturation and aggregation. Molecular chaperones have been classified into five different classes based on the molecular weight, HSP 60, HSP 70, HSP 90, HSP 100 and small HSP (Giessler et al., 2001).

The main function of the HSP 70 is to interact with the unfolded proteins in an ATP dependent manner. This interaction with the unfolded proteins helps in stabilizing the unfolded proteins and helps in refolding of these proteins by preventing aggregation. The abundant form of HSP 70 is found in the mitochondria and termed as the mitochondrial HSP 70 (mtHSP 70) (Giessler et al., 2001). HSP 70 also plays a vital role in the translocation of polypeptides,

required during the formation of the mitochondrial complexes. There was a proposal that the polypeptides are translocated through a channel called the translocation channel, present in the mitochondrial matrix and the polypeptide movement in this channel is generated by Brownian motion (Watcher et al., 1994). As the polypeptide enters the translocation channel and the binding sites are exposed to the matrix, mtHSP 70 binds to the polypeptide in transit, preventing the backward movement of the polypeptide. The complete translocation of the polypeptide takes place through several binding steps of the polypeptide to mtHSP70. After the translocation is complete, the bound mitochondria-destined proteins are released into the matrix, followed by the folding of the proteins (Voisene et al., 2000).

The HSP 60 chaperone system is required for the newly imported mitochondria-destined proteins. HSP60 helps direct proteins into the inter membrane space of mitochondria. The structure of the HSP 60 is such that there is a central cavity, where the unfolded proteins can be bound (Brett et al., 2003). These proteins can be eventually folded through a confirmation shift of the HSP 60 and ATP hydrolysis. The process of the folding and unfolding requires a co-chaperone, HSP 10 (Elisa et al., 2002). HSP 90 also helps in protein folding; but additionally it can assist in protein degradation (Jacob et al., 1994).

Mitochondrial dysfunction in diseased states

Mitochondrial dysfunction in the nervous system is attributed to different factors (e.g., defects of the respiratory chain, protein importation, and mitochondrial dynamics and programmed cell death) (DiMauro and Davidson, 2005). Disruption or mutations in the mitochondrial DNA and genetic errors leading to major mitochondrial functions have major

deleterious effects the nervous system, including the effect on the motility and distribution of mitochondria (DiMauro and Davidson, 2005).

Disorders caused by mutations in mitochondrial DNA

About 200 mtDNA mutations have been associated with human diseases which affect the central and peripheral nervous systems (Tanji et al., 2001). Most of the pathogenic mtDNA mutations are heteroplasmic and the severity of the syndromes they cause differs in different families or in members of the same family (Bykhovskaya et al., 2004). Both mtDNA mutations and rearrangements of the mtDNA in rRNA and tRNA genes impair mitochondrial protein synthesis and ATP production (Hays et al., 2006). Especially in the peripheral nervous system, neurodegenerative disorders like the Kearns-Sayre Syndrome (KSS), Leber hereditary optic neuropathy (LHON) etc and mitochondrial encephalomyopathy (MELAS), myoclonus epilepsy ragged-red fibers (MERRF) etc in central nervous system are associated with mtDNA deletion (Hays et al., 2006). MELAS shows 3243-MELAS mtDNA mutations in the walls of cerebral arteriols and MERRF shows 8344-MERRF mutations in the olivary nucleus of cerebellum (Tanji et al., 2000 and 2001).

The fact that the mutations in different tRNA genes have different mechanism of action and the mechanism of what directs each mutation to a particular area of brain and how the syndromes differ from each other with different clinical manifestation are still poorly understood (Hirano et al., 2006). However, difference in several genes and multiple mtDNA deletions can be involved in several parts of the central and the peripheral nervous systems. Notably the disorders associated with the mutations of adenosine nucleoside translocator (ANT1) and polymerase

gamma (POLG) are associated with mitochondrial neurogastrointestinal encephalomyopathy (MNGIE), peripheral neuropathy, parkinsonism, myoclonus epilepsy, etc. (Nishino et al., 1999).

Several studies have documented that POLG mutations predominantly cause deletions and depletion of the mtDNA and the degree of depletion varies in different tissues (Nishino et al., 1999). The depletion of the mtDNA with mutation in POLG can be attributed in part to mutations in genes encoding deoxyguanosine kinase (dGK), thymidine kinase (TK2), cytosolic p-53 inducible ribonucleotide reductase small subunit (p53R2).

The translation of the 13 mtDNA-encoded subunits of the respiratory chain not only requires the intact mtDNA but also availability of nucleotide building blocks, ribosomal proteins and polymerase (Valente et al., 2007). Defects in mtDNA translation results in respiratory chain complex defects and defective pseudouridylation of mitochondrial tRNA can cause myopathy, lactic acidosis and sideroblastic anemia (MLASA) (Bykhovskaya et al., 2004).

Mitochondrial disorders can also be due to mutations affecting the lipid milieu of the respiratory chain (Gohil et al., 2004). The respiratory chain complexes are embedded in the lipid milieu of the inner mitochondrial membrane, whose major component is cardiolipin (Gohil et al., 2004). The biosynthesis of cardiolipin and the functionality of the respiratory chain are interlinked (Hirano et al., 2006). Apart from scaffolding proteins, cardiolipin is also important for the assembly of the respiratory chain complexes by direct interaction with COX (Hays et al., 2006). Therefore, mutations and abnormalities in cardiolipin can impair the function of respiratory chain (Tanji et al., 2001). One such disorder linked to the mutations in cardiolipin is the Barth Syndrome characterized by mitochondrial myopathy, cardiomyopathy, growth retardation etc. (Gohil et al., 2004). It is caused by the mutation in a phospholipid, tafazzin

(TAZ), that regulates structural and functional integrity of cardiolipid. Mutations in TAZ ultimately lead to altered concentration and composition of cardiolipin thereby affecting the mitochondrial function (Gohil et al., 2004).

Mitochondrial disorders caused by mutations nuclear DNA

The most common mutations in nuclear DNA (nDNA) take place in complex I and complex II and the most manifested syndrome in the population at large is Leigh syndrome (Kirby et al., 2004). The clinical symptoms of this neurodegenerative disorder include vascular proliferation, neuronal loss and demyelination in the basal ganglia and brain stem (Kirby et al., 2004). Other neurodegenerative disorders include LHON, caused by the mutations in both nuclear and mitochondrial DNA, maternally inherited Leigh syndrome (MILS), caused by the mutations in proteins that are not a part of the respiratory complexes but are needed to synthesize and properly assemble the nDNA- and mtDNA-encoded subunits (Alexander et al., 2000). Other neurodegenerative disorders (e.g., Leigh Syndrome-French-Canadian type (LSFC), COX deficient form of LS, nephrotic syndrome (NS) etc.) are associated with mutations in the COX-assembly genes and deficiency of primary coenzyme Q10 (CoQ10) (Schon et al., 2007). CoQ10 transfers electrons from complex I and II to complex II of respiratory chain and receives electrons from the β -oxidation pathway of long-chain fatty acids (Alexander et al., 2000). Deficiency in CoQ10 can block this pathway. Several other syndromes associated with CoQ10 deficiency include autosomal recessive cerebellar ataxia, oculo-motor apraxia, etc. (Alexander et al., 2000). Various other mutations in other complexes manifesting several forms of myopathies have been identified (e.g., the mutations in assembly factor BCS1L for complex III and ATPAF2 for complex V) (Alexander et al., 2000).

More than 1300 proteins have been identified in mammalian mitochondria, only 13 of which are encoded by mtDNA and the rest are encoded by nuclear DNA (Schon et al., 2007). All proteins are synthesized in the cytoplasm and imported into the nucleus and/or mitochondria.

Mitochondrial targeting of proteins is a complex process in lieu of the four compartments of the mitochondria. The mitochondrial proteins are targeted through the interactions between the import machinery, which consists of the heat shock proteins (HSPs) and other chaperones, sorting and assembly machinery (SAM), pre-sequence-associated translocation associated motor (PAM) and mitochondrial import and assembly (MIA) systems. The HSPs require two other proteins, translocase of inner membrane and translocase of outer membrane (TIM and TOM), for unfolding and refolding of mitochondria-targeted proteins (Gabriel et al., 2006). But, fortunately, the mitochondrial disorders associated with the protein import into mitochondria are very rare (Hansen et al., 2002). One such syndrome is an autosomal dominant form of hereditary spastic paraplegia, which is due to the mutations in import chaperonin HSP60 (Hansen et al., 2002). However, more research is needed to identify such disorders in the near future (Hansen et al., 2002).

Mitochondrial disorders can also be caused by disruption in the mitochondrial dynamics. Mutations in OPA-1, which is an inner membrane fusion protein, have been associated with the autosomal dominant optic atrophy (DOA) (Deletre et al., 2000). OPA-1 interacts with mitofusins (Mfn-1 and Mfn-2) to promote mitochondrial fusion (Hirano et al., 2006). Mutations in Mfn-2 cause Charcot Marie Tooth disease (CMT type 2A) (Chung et al., 2006). The other variant forms of this disorder (i.e., CMT type 4A and CMT type 6A) are linked with the mutations in genes encoding ganglioside-induced differentiation protein-1 (GDAP-1) and Mfn-1 (Tanji et al., 2001).

Changes in mitochondrial dynamics can cause impaired mitochondrial motility, which leads to peripheral and optic neuropathy (Chung et al., 2006; Suchner et al., 2006).

Goals, scope and working hypothesis of my thesis research

My thesis project focuses on “Mitochondrial DNA depletion and its effects on mitochondrial dynamics.” The key research question I intend to address is, “What effects does mitochondrial DNA depletion have on the maintenance of mitochondrial functional integrity and how do disease states (e.g., neurodegenerative diseases) disrupt the mechanistic and functional coordination between nDNA-encoded proteins and mtDNA- encoded proteins (i.e., the so-called ‘inter-genomic communication’)?” Within the framework of this research question, I have formulated the general hypothesis that chronic mtDNA deletion induces changes in mitochondrial dynamics and disruption of communication between mitochondrial and nuclear genomes.

To address this hypothesis, we employed dorsal root ganglion (DRG) neurons harboring mtDNA depletions induced by treatment with a low level of ethidium bromide (King and Attardi, 1989; Isaac et al., 2007; Isaac, 2007; Idikuda, 2013) to (i) investigate the putative changes in expression of several key metabolic enzymes and antioxidant enzyme proteins, (ii) determine the mechanisms underlying the changes in mitochondrial dynamics induced by mtDNA deletion; and (iii) elucidate some of the putative mechanisms underlying the disruption of the communication between nDNA and mtDNA induced by mtDNA deletion. The studies to address the general hypothesis are described in detail in Chapters 2 and 3. I contributed to some of the studies in Chapter 2, especially those related to mechanisms underlying mtDNA deletion-

induced disruption of mitochondrial dynamics while the studies detailed in Chapter 3 constitute the bulk of my M.S. thesis research.

In addition to the studies reported in Chapters 2 and 3, I have also participated in two other collaborative projects (one on nanotoxicology of metallic oxide nanoparticles; the other on the effects of glycolytic enzyme inhibitors on cell death mechanisms in human neuroblastoma and astrocytoma cells) of Dr. Lai's laboratory as part of my further training in research in areas other than my major interest in neuroscience. Some of the findings of these participated have been published in a proceedings paper presented in Nanotech 2014 (Lai et al., 2014) and in an abstract of a paper presented at the Annual Meeting of the American Association for Cancer Research (Bhushan et al., 2014). However, discussion of these collaborative projects (see Lai et al., 2014 and Bhushan et al., 2014 for details) that I have participated in is beyond the scope of this thesis.

References

Alexander C, Votruba M, Pesch UEA, Thiselton DL, Mayer S (2000). OPA1, encoding a dynamin-related GTPase, is mutated in autosomal dominant optic atrophy linked to chromosome 3q28. *Nat Genet.* 26:211–215.

Alirol E, James D, Huber D, Marchetto A, Vergani L, Martinou JC, Scorrano L (2006). The mitochondrial fission protein hFis1 requires the endoplasmic reticulum gateway to induce apoptosis. *Biol Cell.* 17(11):4593-4605.

Anand R (2014). OPA1's shortcut to mitochondrial fission. *J Cell Biol.* 204(6):858- 865.

Archer SL (2013). Mitochondrial dynamics — mitochondrial fission and fusion in human diseases. *N Engl J Med.* 369:2236-2251.

Benard G, Karbowski M (2009). Mitochondrial fusion and division: regulation and role in cell viability. *Semin Cell Dev Biol.* 20(3):365-74.

Bhushan A, Chatterji T, Wong YYW, Rizvi N, Balaraju AK, Neti A, Lai JCK (2014) Iodoacetate and 3-bromopyruvate exert differential effects on human neurotumor SK-N-SH and U-87 cells. Annual Meeting of American Association for Cancer Research, April 5-9, 2014, San Diego, CA (in Abstracts Volume).

Bukau B, Horwich AL (1998). The Hsp70 and Hsp60 chaperone machines. *Cell.* 92:351-366.

Bykhovskaya Y, Casas KA, Mengesha E, Inbal A, Fischel-Ghodsian N (2004). Missense mutation in pseudouridine synthase 1 (PUS1) causes mitochondrial myopathy and sideroblastic anemia (MLASA). *Am J Hum Genet.* 74:1303–1308.

Cabiscol E, Bellí G, Tamarit J, Echave P, Herrero E, Ros J (2002). Mitochondrial Hsp60, resistance to oxidative Stress, and the labile iron pool are closely connected in *saccharomyces cerevisiae*. *J Biol Chem.* 227:4531-4538.

Cadenas E, Davies KJ (2000). Mitochondrial free radical generation, oxidative stress, and aging. *Free Radic Biol Med.* 29(3-4):222-2230.

Chan DC (2012). Fusion and Fission: interlinked processes critical for mitochondrial health. *Annu Rev Genet.* 46:265-287.

- Chen H, Chan DC (2009). Mitochondrial dynamics—fusion, fission, movement, and mitophagy—in neurodegenerative diseases. *Hum Mol Genet.* 18:169–176.
- Chung KW, Kim SB, Park KD, Choi KG, Lee JH (2006). Early onset severe and late-onset mild Charcot-Marie-Tooth disease with mitofusin 2 (MFN2) mutations. *Brain.* 129:2103–2118.
- Clark JB, Lai JCK (1989) Glycolytic, tricarboxylic acid cycle and related enzymes in brain. In *NeuroMethods*, Vol. 11 (Boulton AA, Baker GB & Butterworth RF, eds.), pp. 233-281, Humana, Clifton, NJ.
- Cooper GM, Sunderland MA (2000). *The Cell: A molecular approach*, 2nd edition Sinauer Associates, Sunderland, MA.
- Delettre C, Lenaers G, Griffoin JM, Gigarel N, Lorenzo C (2000). Nuclear gene OPA1, encoding a mitochondrial dynamin-related protein, is mutated in dominant optic atrophy. *Nat Genet.* 26:207–210.
- Ferrier V (2001). Mitochondrial fission in life and death. *Nat Cell Biol.* 10:1021-1038.
- Frank S, Gaume B, Bergmann-Leitner ES, Wolfgang W, Leitner, Robert EG, Catez F, Smith CL (2001). The role of dynamin-related protein 1, a mediator of mitochondrial fission, in apoptosis. *Dev Cell.* 1(4):515-525.
- Frey TG, Mannella CA (2000). The internal structure of mitochondria structure and dynamics of the mitochondrial inner membrane cristae. *Trends Biochem Sci.* 25(7):319-324.
- Gabriel K, Milenkovic D, Chacinska A, Muller J, Guiard B (2006). Novel mitochondrial intermembrane space proteins as substrates of the MIA import pathway. *J Mol Biol.* 365:612–620.

Geissler A, Rassow J, Pfanner N, Voos W (2001). Mitochondrial import driving forces: enhanced trapping by matrix hsp70 stimulates translocation and reduces the membrane potential dependence of loosely folded preproteins. *Mol Cell Biol.* 21:7097-7104.

Geissler A, Krimmer T, Bomer U, Guiard B, Rassow J, Pfanner N (2000). Membrane potential driven protein import into mitochondria: the sorting sequence of cytochrome b (2) modulates the delta psi-dependence of translocation of the matrix-targeting sequence. *Mol Biol Cell.* 11:3977-3991.

Gohil VM, Hayes P, Matsuyama S, Schagger H, Schlame M, Greenberg ML (2004). Cardiolipin biosynthesis and mitochondrial respiratory chain function are interdependent. *J Biol Chem.* 279:42612–45618.

Gredilla R (2011). DNA Damage and base excision repair in mitochondria and their role in aging. *J Aging Res.* 25:70-93.

Hackenbrock CR (1966). Reversible ultrastructural changes with change in metabolic steady state in isolated liver mitochondria. *J Cell Biol.* 30(2):269-297.

Hansen JJ, Durr A, Cournu-Rebeix I, Georgopoulos C, Ang D (2002). Hereditary spastic paraplegia SPG13 is associated with a mutation in the gene encoding the mitochondrial chaperonin Hsp60. *Am J Hum Genet.* 70:1328–1332.

Idikuda VK (2013). Mitochondrial dynamics in Schwann cells and dorsal root ganglion neurons. M.S. Thesis, Idaho State University, Pocatello, Idaho.

Irshad M and Chaudhuri PS (2002). Oxidant and antioxidant-role and significance in human body. *Ind J Exp Biol.* 42:1233-1239.

Isaac AO (2007). Mitochondrial DNA depletion alters energy metabolism, antioxidant systems, and intergenomic signaling: implications in neurodegeneration, toxicity to nucleoside analogue-based HIV therapy and mitochondrial myopathies. Ph.D. Dissertation, Idaho State University, Pocatello, Idaho.

Isaac AO, Dhukande VV, Lai JCK (2007). Metabolic and antioxidant system alterations in astrocytoma cell line challenged with mitochondrial DNA deletions. *Neurochem Res.* 11:1906-1918.

Kasashima K, Nagao Y, Endo H (2014). Dynamic regulation of mitochondrial genome maintenance in germ cells. *Reprod Med Biol.* 13:11–20.

Kaufman BA, Kolesar JE, Perlman PS, Butow RA (2003). A function for the mitochondrial chaperonin HSP60 in the structure and transmission of mitochondrial DNA nucleoids in *Saccharomyces cerevisiae*. *J Cell Biol.* 163(3):457-461.

Kharb S, Singh V (2004). Nutraceuticals in health and disease prevention. *Ind J Clin Biochem.* 19(1):50–53.

Kienhöfer J, Franziska DJ, Ruckelshausen F, Muessig E, Weber K, Pimentel D, Ullrich V, Bürkle A, Bachschmi M (2009). Association of mitochondrial antioxidant enzymes with mitochondrial DNA as integral nucleoid constituents. *FASEB J.* 23(7):2034–2044.

Kirby DM, Boneh A, Chow CW, Ohtake A, Ryan MT (2003). Low mutant load of mitochondrial DNA G13513A mutation can cause Leigh's disease. *Ann Neurol.* 54:473–478.

Krauss S (2001). Mitochondria: structure and role in respiration. *Encyclopedia of Life Sciences.* Nature Publishing Group. New York City, NY.

Lai JCK (1992) Oxidative Metabolism in Neuronal and Non-Neuronal Mitochondria. *Can J Physiol Pharmacol.* 70:S130-S137.

Lai JCK, Clark JB (1989). Isolation and characterization of synaptic and non-synaptic mitochondria from mammalian brain. In *NeuroMethods*, Vol. 11 (Boulton AA, Baker GB & Butterworth RF, eds.), pp. 43-98, Humana, Clifton, NJ.

Lai JCK, Balaraju AK, Neti A, Lai MB, Tadinada SM, Idikuda, VK, Singh MRM, Mukka K, Pfau J, Bhushan A, Leung SW (2014) Zinc oxide nanoparticles induced apoptosis and necrosis in human neuroblastoma and astrocytoma cells. In *Technical Proceedings of the 2014 NSTI Nanotechnology Conference & Expo, Nanotech 2014 Vol. 3, section 2. Sustainable Nanotechnology: Environmental Apps. & EHS Implications*, pp. 138-141.

Lai JCK, Lai MB, Jandhyam S, Dukhande VV, Bhushan A, Daniels CK, Leung SW (2008). Exposure to titanium dioxide and other metallic oxide nanoparticles induces cytotoxicity on human neural cells and fibroblasts. *Int J Nanomed.* 3(4): 533-545.

Lee HC, Weh YH (2007). Oxidative stress, mitochondrial DNA mutation and apoptosis in aging. *Exp Biol Med.* 232(5):592-606.

Liesa M, Palacín M, Zorzano A (2008). Mitochondrial dynamics in mammalian health and disease. *Physiol Rev.* 89:799-845.

Mannella CA, Buttle K, Marko M (1997). Reconsidering mitochondrial structure: new views of an old organelle. *Trends Biochem Sci.* 22:37–38.

Mannella CA (2006). Mitochondrial dynamics in cell life and death. *Molecular Cell Research.* 1763(5–6):542–548.

Moraes CT, Kenyon L, Hao H (1999). Mechanisms of human mitochondrial DNA maintenance: the determining role of primary sequence and length over function. *Mol Biol Cell*. 10:3345–3356.

Nishino I, Spinazzola A, Hirano M (1999). Thymidine phosphorylase gene mutations in MNGIE, a human mitochondrial disorder. *Science*. 283:689–692.

Otera H, Mihara K (2011). Molecular mechanisms and physiologic functions of mitochondrial dynamics. *J Biochem*. 149(3): 241-251.

Ott M, Gogvadze V, Orrenius S, Zhivotovsky B (2007). Mitochondria, oxidative stress and cell death. *Apoptosis*. 12:913–922.

Peng C, Wang X, Chen J, Jiao R, Wang L, Li YM, Zuo Y, Liu Y, Lei L, Ma KY, Huang Y, Chen ZY (2014). Biology of aging and role of dietary antioxidants. *Biomed Res Int*. 14: 831-841.

Picard M, Taivassalo T, Gouspillou G, Hepple RT (2011). Mitochondria: isolation, structure and function. *J Physiol*. 589: 4413-4421.

Rassow J, Ahsen OV, Bomer U, Pfanner N (1997). Molecular chaperons: towards a characterization of the heat shock protein 70 family. *Trends Cell Biol*. 7: 129-133.

Ranieri M, Brajkovic S, Riboldi G, Ronchi D, Rizzo F, Bresolin N, Corti S, Comi GP (2011). Mitochondrial fusion proteins and human diseases. *Neurol Res Int*. 55: 89-93.

Schon EA, Rizzuto R, Moraes CT, Nakase H, Zeviani M, DiMauro S (1989). A direct repeat is a hotspot for large-scale deletions of human mitochondrial DNA. *Science*. 244:346–349.

Scott I, Youle RJ (2010). Mitochondrial fission and fusion. *Essays Biochem*. 47:85-98.

Shadel GS, Clayton DA (1997). Mitochondrial DNA maintenance in vertebrates. *Annu Rev Biochem.* 66:409-435.

Shadel GS (2008). Expression and maintenance of mitochondrial DNA: new insights into human disease pathology. *Am J Pathol.* 172:106-111.

Shokolenko I, LeDoux S, Wilson G, Alexeyev M (2002). In mitochondrial function and dysfunction. Chapter 16. pp: 339-350.

Stuart JA, Brown MF (2006). Mitochondrial DNA maintenance and bioenergetics. *Biochim Biophys Acta.* 72:79–89.

Van der Bliek AM, Shen Q, Kawajiri S (2013). Mechanisms of mitochondrial fission and fusion. Cold Spring Harbor Laboratory Press. 10:1101-1107.

Valente L, Tiranti V, Marsano RM, Malfatti E, Fernandez-Vizarra E (2007). Infantile encephalopathy and defective mitochondrial DNA translation in patients with mutations of mitochondrial elongation factors EGF1 and EFTu. *Am J Hum Genet.* 80:44–58.

Von Ahsen O, Voos W, Henninger H, Pfanner N (1995). The mitochondrial protein import machinery: Role of ATP in dissociation of Hsp70, Mim44 complex. *J Biol Chem.* 270:848-853.

Wallace DC (2007) Why do we still have a maternally inherited mitochondrial DNA? Insights from evolutionary medicine. *Annu Rev Biochem.* 76:781-821.

Watcher C, Schatz G, Glick BS (1994). Protein import into mitochondria: the requirement for external ATP is precursor specific whereas intra mitochondrial ATP is universally needed for translocation into the matrix. *Mol Biol Cell.* 5:465-474.

Zuchner S, Mersiyanova IV, Muglia M, Bissar-Tadmouri N, Rochelle J, Dadali EL, Zappia M, Nelis E, Patitucci A, Senderek J, Parman Y, Evgrafov O, Jonghe PD, Takahashi Y, Tsuji S, Pericak-Vance MA, Quattrone A, Battaloglu E, Polyakov AV, Timmerman V, Schroder JM, Vance JM (2004). Mutations in the mitochondrial GTPase mitofusin 2 cause Charcot-Marie-Tooth neuropathy type 2A. *Nat Genet.* 36(5): 449-451.

Chapter 2

Differential Effects of Chronic Mitochondrial DNA Deletion on Metabolism and Mitochondrial Dynamics in Dorsal Root Ganglion Neurons and Schwann Cells

Vinay K. Idikuda¹, Aishwarya Neti¹, Anurag K. Balaraju¹, Alfred O. Isaac², Alok Bhushan³ and James C.K. Lai¹

¹Department of Biomedical & Pharmaceutical Sciences, College of Pharmacy, Division of Health Sciences and Biomedical Research Institute, Idaho State University, Pocatello, ID 83209, USA

²Department of Pharmaceutical Sciences and Technology, School of Health Sciences and Technology, Technical University of Kenya, Nairobi, Kenya

³Department of Pharmaceutical Sciences, Jefferson School of Pharmacy, Thomas Jefferson University, Philadelphia, PA 19107, USA

Abstract

Mitochondrial DNA mutations and/or deletions have been noted in chronic neurodegenerative diseases such as Alzheimer's and Parkinson's disease. These defects lead to impaired activities of metabolic enzymes and induce oxidative stress. Hence we have developed cell models to study the changes that occur in the cells devoid of mitochondrial DNA. In this study, we have employed ethidium bromide for depleting mitochondrial DNA, which severely affected the expression of vital metabolic enzymes such as hexokinase, lactate dehydrogenase, citrate synthase and malate dehydrogenase. Our results suggested cells devoid of mitochondrial DNA adapted by increasing their capacity of glycolysis to compensate for their lower capacity in tricarboxylic acid cycle metabolism. In addition, our results also indicated that DRG neurons were more susceptible to deletion of their mitochondrial DNA and oxidative stress compared to Schwann cells. Thus, our study provides unique neural cell models for analyzing metabolic changes that occur in cells harboring mtDNA deletions. Thus, our findings may have pathophysiological implications in peripheral neuropathies in particular and neurodegeneration in general.

Keywords: mitochondrial DNA deletion and depletion, metabolic changes and adaptation, oxidative stress, mitochondrial dynamics, peripheral neuropathy, neurodegeneration.

Introduction

Mitochondria are dynamic organelles that regulate a wide variety of cellular functions such as cellular respiration, apoptosis, managing oxidative stress and maintenance of calcium homeostasis (Rousset et al., 2004). Mitochondria contain enzymes required for proper functioning of tricarboxylic acid (TCA) cycle, fatty acid oxidation, and pyruvate oxidation and also possess multiple copies of mitochondrial genome per mitochondrion. The mitochondrial genome contains 37 genes which encode for 13 mitochondrial polypeptides, apart from the rRNAs and tRNAs (Chacinska et al., 2009). However approximately 1500 nuclear encoded genes are required for the proper functioning of mitochondria (Kim et al., 2008). Many mitochondrial disorders originate from defects in the mitochondrial genome (DiMauro and Bonilla, 1997). Since the mitochondrial DNA encodes for 13 polypeptides which are component parts of four of the five respiratory chain complexes, these disorders can be, at least in part, attributed to the dysfunction of the respiratory chain consequent to mitochondrial DNA defects. The disorders such as myoclonus epilepsy with ragged red fibers (MERRF), mitochondrial myopathy, encephalopathy, lactic acidosis, and stroke-like episodes (MELAS), and Leber's hereditary optic neuropathy (LHON) are due to the deletions in the mitochondrial DNA (DiMauro and Bonilla, 1997).

Mitochondrial dysfunction can also be manifested in different neurodegenerative disorders (e.g., Parkinson's disease (PD), Huntington's disease (HD), and Alzheimer's disease (AD)) (Beal, 2005). AD is the most common type of neurodegenerative disorder in the central nervous system and has been characterized by decreased oxidative metabolism in both the peripheral and central nervous systems (Gibson et al., 1998). Three key enzymes of tricarboxylic acid cycle have been impaired in AD: these include pyruvate dehydrogenase complex, isocitrate

dehydrogenase and α -ketoglutarate dehydrogenase complex (Gibson et al., 1998; Bubber et al., 2005). However, in the case of PD, a deficiency of complex I of the electron transport chain has been noted, apart from the loss of dopaminergic neurons, which is the key hall mark of PD (Beal, 2007). As stated above there is strong evidence supporting mitochondrial dysfunction in neurodegenerative diseases, and in a number of instances, there is a direct involvement of mitochondrial DNA (mtDNA) in neurodegenerative diseases such as AD and Friedreich's ataxia (Beal, 2005).

In view of the implication of mtDNA aberrations in neurodegenerative diseases discussed above, there is need for neural cellular models harboring mtDNA deletion to facilitate the elucidation of the role of mtDNA in neurodegenerative diseases because such cell models can closely mimic the mtDNA aberrations noted in many – if not all – neurodegenerative diseases. Moreover, very few studies to date have addressed the implications of mitochondrial DNA depletion in peripheral neuropathy: this critical gap in our knowledge can be attributed to the lack of appropriate neural cell models derived from the peripheral nervous system (PNS).

Previous studies from our laboratory have documented the implications in mitochondrial myopathy and alterations in antioxidant system and intergenomic signaling in the U87 (human astrocytoma) cell line challenged with mitochondrial DNA deletion (Isaac, 2007). Few other studies have reported metabolic and antioxidant changes in mitochondrial DNA depletion and its implication in peripheral neuropathy (Isaac et al., 2007). Hence in this study, we have aimed at developing in vitro cell culture model devoid of the mitochondrial DNA and to determine the effect of mitochondrial DNA depletion on energy metabolism, antioxidant changes and mitochondrial dynamics.

Materials and Methods

Materials

Ethidium bromide was purchased from Sigma Aldrich (St. Louis, MO), Dialyzed FBS was purchased from Atlanta Biologicals (Norcross, GA), Tween 20, sodium pyruvate, Dulbecco's Modified Eagle media (DMEM), L-glutamine, phenol red from Sigma (St. Louis, MO), SDH anti-mouse antibody from Santa-cruz biotechnology (Santa Cruz, CA), Mitofusin, Manganese superoxide dismutase antibodies were purchased from Abcam antibodies (Cambridge, MA). Hexokinase II and ND6, cytochrome-c-oxidase-2 antibodies were purchased from Molecular Probes (Eugene, OR). The chemiluminescence reagents and bicinchoninic protein assay (BCA) kit were obtained from Thermo Fisher (Waltham, MA); and autoradiography films were from Biomax (Rochester, NY). Protease inhibitor cocktail tablets were from Roche diagnostics (Mannheim, Germany) and Mitotracker red dye was purchased from Invitrogen (Carlsbad, CA). Except otherwise stated, all other chemicals used were purchased from Sigma Aldrich (St. Louis, MO).

Cell Culture

Immortalized dorsal root ganglion (DRG) neurons were a generous gift from Dr. Ahmet Höke (Johns Hopkins University School of Medicine) (Chen et al., 2007) and R3 (neuronal Schwann cell; immortalized with SV40 large T antigen) was acquired from ATCC (Manassas, VA, USA). Both cell lines were cultured in DMEM medium supplemented with 10% (v/v) dialyzed fetal bovine serum (Atlanta Biologicals, Norcross, GA), 100 µg/ml uridine, 1% (w/v) sodium pyruvate, 0.292 g/L L-glutamine, 1.5 g/L sodium bicarbonate, and 4.53 g/L glucose

(Sigma Aldrich, St. Louis, MO). The cell lines were treated with 50 ng/ml ethidium bromide (Sigma Aldrich, St. Louis, MO) over a period of 15 weeks to deplete their mitochondrial DNA. The cells were allowed to grow to 70% confluent before being used for all the experiments mentioned hereafter and maintained at 5% (v/v) carbon dioxide and at 37°C.

Western Blot Analysis

DRG neurons or Schwann cells were seeded in a T-75 flask and were incubated until 70% confluent. To prepare lysates, cells were washed in ice-cold 1X phosphate-buffered saline (PBS) thrice and harvested by using the lysis buffer containing Tris, sodium chloride, glycerol, EDTA, protease inhibitor cocktail, phenylmethylsulfonyl fluoride (PMSF) and sodium orthovanadate. The washed cells were collected and homogenized by sonications. The sonicated samples were then centrifuged at ~15,000 g for 10 min at 4°C. The resultant supernatant was collected and to it was added 2 X lammeli buffer. The samples were heated at 90°C for 5 minutes and stored at -80°C. The proteins in the samples so prepared were separated by sodium dodecyl sulfate- polyacrylamide gel electrophoresis (SDS-PAGE) using 10% (w/v) gels. The separated proteins were then transferred onto a polyvinylidene difluoride (PVDF) membrane and were blocked by using 5% (w/v) milk powder solution for an hour at room temperature. These blots were then washed with Tris-buffered saline (TBS) and incubated with the desired primary antibody overnight. The blots were then washed using TBS and incubated with HRP-conjugated secondary antibody for an hour and developed using chemiluminescence.

Cells Studied with Confocal Microscopy

DRG neurons were cultured in DMEM medium containing ethidium bromide to generate cells devoid of mitochondrial DNA as described above. They were harvested and plated for

confocal microscopy in a 6-well plate and the cells were then allowed to grow on a microscopic slide sterilized with ethanol. After the cells had attached to the slide, they were incubated with 500 nm Mitotracker deep red for 40 minutes at 37°C for the dye to permeabilize and stain the cells' mitochondria. Then the excess dye was removed and the slides were washed thrice with PBS. The washed cells were then fixed with 4% paraformaldehyde for 20 minutes. The cells were again washed with PBS. Subsequently, coverslips were mounted onto the glass slides using anti-fade reagent. Images of stained cells were acquired using a confocal microscope (Olympus FV1000 confocal microscope) with a 60x oil-immersion objective and at 1024 x 1024 resolutions. Confocal Z-stacks were acquired over 30 minutes and the photomicrographs were chosen at an optimum z-step.

BCA Protein Assay

Equal numbers of cells were plated in T-75 flasks and cells devoid of mitochondrial DNA were generated by treating them with ethidium bromide as described above. When they were ~70% confluent, the cells were harvested and lysate was prepared using lysis buffer as described above. Then the sonicated cell lysate was centrifuged and the resultant supernatant fraction was collected as described above and stored. The protein content of the supernatant fractions was determined employing the BCA protein Assay kit (Fischer Thermo Scientific, Waltham, MA) as described previously (Dukhande et al., 2013).

Flow Cytometry

A Benton Dickinson FACS caliber flow cytometer was used to estimate the mitochondrial mass in the control and ethidium bromide-treated cells. The cells were grown in T75 flasks, the treated cells were treated with 50 ng/ml of ethidium bromide for 14 weeks and

were supplemented with sodium pyruvate and uridine. After attaining 75% confluence, the cells were incubated with 300 nM (the stock solution was prepared in DMSO and was diluted to required concentration using pre-warmed medium) Mitotracker green (Molecular Probes, OR) at 37°C and humidified atmosphere of 5% (v/v) CO₂. After 30 minutes, the cells were harvested by trypsinization after having been washed thrice with ice-cold PBS. The fluorescence of the stained cells was measured at 412 nm: their total fluorescence was proportional to the mitochondrial mass in the stained cells.

Preparation of Cell Homogenates and Enzyme Assays

DRG neurons and Schwann cells were grown in DMEM culture medium containing ethidium bromide (50 ng/ml) for 14 weeks to generate ρ^0 cells: their medium was also supplemented externally with uridine and sodium pyruvate as detailed above.

Preparation of cell homogenates. DRG neurons or Schwann cells were seeded equally in 3 T75 flasks and grown to 70% confluency; the culture medium was then discarded and the cells were washed three times with ice cold PBS. The cells were harvested by scraping and collected in 5 ml PBS. The cell suspension was then centrifuged at 1000 x g for 10 minutes and the resultant supernatant was discarded and then the pellet was homogenized using a Dounce homogenizer with homogenizing buffer (0.25 M Sucrose and 0.5 mM HEPES-Tris pH 7.4 + protease inhibitor cocktail) until a clear homogenate was obtained. Part of the homogenate was used to estimate the protein content. Protein analysis for lysates was performed using the bicinchoninic acid assay (BCA) kit (Pierce, USA) employing a microplate reader at 562 nm.

Hexokinase assay. Hexokinase is the first enzyme of the glycolytic pathway; it is assayed by coupling glucose-6-phosphate production to NADP⁺ reduction in presence of

glucose-6-phosphate dehydrogenase (Clark and Lai, 1989). The assay mixture consisted of 0.1 M MOPS-Tris pH 7.8, 0.1 % (v/v) Triton-X, 8 mM MgCl₂, 0.4 mM NADP⁺, 5 mM D-glucose, and 5 units of yeast glucose-6-phosphate dehydrogenase. The final volume in the cuvette was 1 ml and 80 µl of homogenate was used and the volume was made up with water. A blank reading was performed at first (without ATP). The reaction is initiated by adding 1 mM ATP. The linear rate of reduction of NADP⁺ was measured at 340 nm for 5 minutes using an Agilent-8453 UV-Vis spectrophotometer. An initial lag of 1 minute was observed in this assay. The blank rate was subtracted from the rate of reaction and the specific activity of the enzyme was then calculated.

Lactate dehydrogenase assay. Lactate dehydrogenase converts pyruvate to lactate, simultaneously oxidizing NADH. Rate of NADH oxidation was monitored at 340 nm for 180 seconds using an Agilent-8453 UV-Vis spectrophotometer (Clark and Lai, 1989). The assay mixture contained 0.1 M potassium phosphate buffer (pH 7.4), 0.5 % (v/v) Triton X-100, 0.25 mM NADH and 1.65 mM sodium pyruvate. The reaction was initiated by addition of NADH. Final volume in the cuvette was adjusted to 1 ml.

Citrate synthase assay. Citrate synthase activity was measured by the rate of formation of free CoA from acetyl CoA (Clark and Lai, 1989). Free CoA reacted with DTNB to give a colored product whose rate of formation was measured at 412 nm for 180 seconds. The assay mixture consisted of 0.1 M Tris-HCl pH 8.0, 0.1 mM oxaloacetate and 0.1 mM DTNB, 0.08% (v/v) Triton X-100, 0.05 mM acetyl CoA and 10 µl homogenate. The reaction was initiated by oxaloacetate addition.

NAD-linked malate dehydrogenase assay. Malate dehydrogenase activity was measured by monitoring the rate of formation of malate from oxaloacetate with simultaneous

oxidation of NADH measured at 340 nm using an Agilent-8453 UV-Vis spectrophotometer (Clark and Lai, 1989). The assay mixture consisted of 0.1 M phosphate buffer pH 7.4, 0.16 mM NADH, 0.16% (v/v) Triton X-100, 0.133 mM oxaloacetate, and 100 μ l tissue homogenate. Oxaloacetate was added last to initiate the reaction (Clark and Lai, 1989).

RESULTS

Generation of ρ^0 cells derived from DRG neurons and Schwann cells

We employed DRG neurons (Chen et al., 2007) and Schwann (R3) cells to produce their corresponding ρ^0 cells by treating the “parent cells” with a low level of ethidium bromide (i.e., 50 ng/ml) for 15 weeks. We (Isaac, 2007; Isaac et al., 2007) and others (Fukuyama et al., 2002; King et al., 1989) have shown that at the low level we employed, ethidium bromide did not appear to affect the nuclear genome. Under bright field light microscopy (Fig. 1), we observed the morphology of the ρ^0 cells appeared to differ from that of their “parent cells.” This difference was particularly noticeable in the case of the ρ^0 cells derived from DRG neurons compared to the ρ^0 cells derived from Schwann cells (Fig. 1). The ρ^0 cells generally appeared to be small and at times “shrunk” (Fig. 1) and grow slower compared to their “parent” cells. The approximate doubling time of Schwann cells was 36 hours and their ρ^0 cells was 72 hours and that of DRG neurons and their ρ^0 cells was 48 hours and 72 hours respectively.

Characterization of the ρ^0 phenotype of DRG neurons and Schwann cells

Both NADH dehydrogenase subunit 6 (ND6) and cytochrome oxidase subunit 2 (COX2) are genes encoded by the mtDNA. Our previous studies on ρ^0 cells from CNS neural cells have

demonstrated that when the expression of ND6 and COX2 was no longer detectable in neural cells chronically treated with ethidium bromide, mtDNA in those cells were completely deleted (Isaac, 2007; Isaac et al., 2007). Consequently, we decided to use these criteria to assess our progress in deleting mtDNA from DRG neurons and Schwann cells as we generated ρ^0 cells from such “parent” cells.

As we treated both DRG neurons and Schwann cells with ethidium bromide, both cell types exhibited time-related decreases in their expression of ND6 (Figs. 2 and 3) and COX2 (Figs. 4 and 5) and after four weeks of treatment with ethidium bromide, expression of ND6 and COX2 were not detectable in both cell types (Figs. 2-5).

Two generalizations can be arrived at based on our findings. (i) The time-related, ethidium bromide-induced disappearance in expression of ND6 occurred sooner than that of COX2. This generalization is consistent with what we had observed in our previous studies on ρ^0 cells generated from U87 cells (Isaac, 2007; Isaac et al., 2007). (ii) The time-related, ethidium bromide-induced disappearance in expression of both ND6 and COX2 occurred sooner in DRG neurons than in Schwann cells.

Succinate dehydrogenase (SDH), a component of the inner mitochondrial membrane respiratory complex II, is encoded by the nuclear genome. We have previously employed the expression of SDH as a negative control for monitoring the generation of ρ^0 cells from U87 cells (Isaac, 2007; Isaac et al., 2007). Consequently, we have also employed SDH expression as the negative control in this study (Figs. 6 and 7). We found that neither DRG neurons nor Schwann cells that were chronically treated with ethidium bromide exhibited any significant decreases in their SDH expression over the four weeks monitored. Thus, these results are compatible with our

earlier observation obtained with ρ^0 cells from U87 cells (Isaac, 2007; Isaac et al., 2007). Furthermore, our results obtained with DRG neurons and Schwann cells chronically treated with ethidium bromide for four weeks (Figs. 6 and 7) suggested that our treatment with ethidium bromide was unlikely to have affected the DNA in the nuclei of DRG neurons and Schwann cells.

Putative changes in mitochondrial mass in the ρ^0 cells

Because we found that mtDNA deletion induced marked changes in the morphology of both DRG neurons and Schwann cells (see above and Fig. 1), we hypothesized that mtDNA deletion induces adaptive changes in mitochondrial structural and function in these two PNS neural cell types. In the first experiment to investigate this hypothesis, we determined cellular mitochondrial mass in DRG neurons and Schwann cells and in their corresponding ρ^0 cells (Fig. 8). MitoTracker Green has been demonstrated to be a useful fluorescent dye for staining mitochondria in live cells so as to facilitate the study of their morphological changes as well as quantitating mitochondrial mass in cells. More importantly and relevant to our application is the fact its staining of mitochondria does not critically depend on the membrane potential of the mitochondria in the cells (Pendergrass et al., 2004). We therefore combined staining of the cells with this dye coupled to flow cytometry to determine the effects of mtDNA deletion on mitochondrial mass in DRG neurons and Schwann cells (Fig. 8).

We found the mean fluorescence intensities in the stained ρ^0 cells of both DRG neurons and Schwann cells were lowered those in their respective “parent” cells stained the same way (Fig. 8). Our results strongly suggest that mtDNA deletion in both cell types induces decreases in

their mitochondrial mass. Furthermore, this effect was much more pronounced in DRG neurons than in Schwann cells (Fig. 8).

Alterations in energy metabolism in the ρ^0 cells derived from PNS neural cells

To further investigate our hypothesis that mtDNA deletion induces adaptive changes in mitochondrial structural and function in DRG neurons and Schwann cells derived from the PNS, we examined the effects of mtDNA depletion on the activities of two tricarboxylic acid (TCA) cycle (namely citrate synthase (CS) and malate dehydrogenase (MDH)) and two glycolytic and related enzymes (namely hexokinase (HK) and lactate dehydrogenase (LDH)) because our previous studies on ρ^0 cells derived from CNS neural cells (i.e., U87 cells) had demonstrated that the activities of such energy-metabolizing enzymes were altered compared to those in their “parent” cells (Isaac, 2007; Isaac et al., 2007).

When we compared the activities of the four energy-metabolizing enzymes studied in ρ^0 cells as compared to their corresponding activities in the control (i.e., their “parent” cells), we found a general trend. The activities of TCA cycle enzymes, namely CS and MDH, were lower in the ρ^0 cells of both DRG neurons and Schwann cells as compared to the corresponding values in their “parent” cells (Figs. 9 and 10) while the opposite trend was observed in the activities of the glycolytic and related enzymes, namely HK and LDH (Figs. 11 and 12), as expected of the ρ^0 cells as they have to rely on glycolysis for their energetic needs. More specifically, when compared to the corresponding activities in their “parent” (i.e., control) cells, CS activities decreased by ~70% ($p < 0.05$) in the ρ^0 cells derived from DRG neurons and decreased by ~30% ($p > 0.05$) in the ρ^0 cells derived from Schwann cells (Fig. 9) whereas MDH activities decreased

by 15% ($p>0.05$) in the ρ^0 cells derived from DRG neurons and decreased by ~40 ($p<0.05$) in the ρ^0 cells derived from Schwann cells (Fig. 10).

On the other hand, when compared to the corresponding activities in their “parent” (i.e., control) cells, HK activities increased by ~30% ($p<0.05$) in the ρ^0 cells derived from DRG neurons and increased by ~540 ($p<0.05$) in the ρ^0 cells derived from Schwann cells (Fig. 11) whereas LDH activities increased by ~200% ($p<0.05$) in the ρ^0 cells derived from DRG neurons and increased by ~40 ($p<0.05$) in the ρ^0 cells derived from Schwann cells (Fig. 12).

Taken together, our results (Figs. 9-12) suggest that energy metabolism in both DRG neurons and Schwann cells adapted to the pathophysiological changes induced by chronic mtDNA deletion. As expected, both cell types adapted by up-regulation of glycolysis (as exemplified by increased activities of HK and LDH) in the absence of functional mitochondrial respiratory chain and electron transport. Additionally, our results also suggest mtDNA deletion exerted differential effects on DRG neurons and Schwann cells.

Alterations of antioxidant system and intergenomic communication

Our previous studies have provided some evidence that chronic mtDNA deletion in astrocytoma (astrocytes-like) U87 cells induces changes in their antioxidant system and disruption of communications between nuclear DNA (nDNA) and mtDNA (Isaac, 2007; Isaac et al., 2007). To investigate the possibility that mtDNA deletion may exert also similar effects on DRG neurons and Schwann cells, we monitored the expression of manganese superoxide dismutase (MnSOD), heat shock protein 70 (HSP70), mitochondrial heat shock protein 70 (mtHSC70), and heat shock protein 90 (HSP90) in DRG neurons and Schwann (R3) cells as they were chronically treated with ethidium bromide.

Our results demonstrated by the time the cells attained their respective ρ^0 phenotype, the expression of MnSOD was increased in ρ^0 cells derived from DRG neurons whereas the expression of MnSOD in ρ^0 cells derived from Schwann (R3) cells did not show any increases (Fig. 13). By contrast, by the time the cells attained their respective ρ^0 phenotype, the expression of HSP70, mtHSP70, and HSP90 decreased in ρ^0 cells derived from DRG neurons (Fig. 14) whereas the expression of HSP70, mtHSP70, and HSP90 did not show any decreases in ρ^0 cells derived from Schwann (R3) cells (Fig.15). Thus, our findings (Figs. 13 and 14) in ρ^0 cells derived from DRG neurons are consistent with the hypothesis that chronic mtDNA deletion induces changes in their antioxidant system and disruption of communications between nuclear DNA (nDNA) and mtDNA. Additionally, our results also suggest that DRG neurons are more susceptible to the effects of mtDNA deletion and oxidative stress than Schwann (R3) cells.

Effect of mtDNA deletion on mitochondrial dynamics

Mitochondrial fusion and fission are important contributors to mitochondrial morphology and function. We investigated the hypothesis that mtDNA deletion induces alteration in mitochondrial dynamics by first examining the effects of mtDNA deletion on the expression of Mitofusin-1 (Mfn-1) and Mitofusin-2 (Mfn-2) in DRG neurons and Schwann (R3) cells. Our results demonstrated that by the time the cells attained their respective ρ^0 phenotype, the expression of Mfn-1 but not Mfn-2 was decreased in ρ^0 cells derived from DRG neurons (Fig. 16) whereas the expression of both Mfn-1 and Mfn-2 in ρ^0 cells derived from Schwann (R3) cells was relatively stable and did not show any decreases (Fig. 17). Thus, our results strongly suggest that mtDNA deletion exerts different effects on mitochondrial dynamics in DRG neurons and Schwann (R3) cells and DRG neurons are more susceptible than Schwann cells to such effects.

To confirm that mtDNA deletion affects mitochondrial dynamics in DRG neurons, we compared mitochondrial dynamics in DRG neurons and the ρ^0 cells derived there from by staining both types of cells with MitoTracker deep red and then examining them under confocal microscopy. Under confocal microscopy, DRG neurons stained with MitoTracker deep red showed many strands/chains of fused mitochondria, especially in the peri-nuclear region of the cytoplasm of these cells (Fig. 18). By contrast, in the ρ^0 cells derived from DRG neurons similarly stained, many fewer strands/chains of fused mitochondria were observed compared to those in their “parent” DRG neurons, instead the mitochondria in the ρ^0 cells appeared to be in small clusters (Fig. 18). Thus, our results employing confocal microscopy (Fig. 18) are consistent with the finding of decreased expression of Mfn-1 in the ρ^0 cells derived from DRG neurons (Fig. 16) and confirmed that mtDNA deletion did induce changes in mitochondrial dynamics in the ρ^0 cells derived from DRG neurons (Fig. 18).

DISCUSSION

Ethidium bromide being a cationic dye predominantly concentrates in the mitochondria and brings about mtDNA depletion (Liang et al., 2001). Owing to its poor defense mechanisms mtDNA is subject to various insults which have deleterious effects if persisted (Vaillant et al., 1991; Nunez et al., 2002). Our study employed chronic ethidium bromide treatment which resulted in shrunken cells with lowered mitochondrial metabolism. The expression of ND6 was lost earlier than COX-2 in both the cell lines; these results complemented those from the previous studies (Pena et al., 1977; Isaac et al., 2006). Because of the nonfunctional ETC, the ATP generation was dependent on glycolysis which was evident with the overexpression of hexokinase 2 in both the cell lines. Nevertheless, mtDNA depletion induced differential effects in both the cell lines: the specific activity of citrate synthase was found to be significantly lowered in DRG neurons whereas the decrease in R3 cells was not found to be significant. On the other hand, MDH specific activity was significantly lowered in R3 but not in DRG neurons. The specific activities of LDH and hexokinase were found to be increased as expected in both the cell lines. Other studies have also reported similar glycolytic shift in p0 cells and described this shift as reversible and respiration dependent. This kind of anaerobic shift decreased mitochondrial metabolism and apoptosis resistance of rho⁰ cells has been thought to simulate cancer phenotype and a potential link to Warburg phenomena (Fukuyama et al., 2002).

Oxidative stress is another major contributor to neurodegeneration. Depletion of mtDNA is known to bring about oxidative stress in neurons which if prolonged leads to cell death. Our results have shown differential effects in both the cell lines under study. DRG neurons have

shown a decreased expression of cytosolic HSP70, mtHSP70 and HSP90 whereas the expression of these proteins was relatively stable in R3 cell line. In addition, although our study did not aim at delineating the differences in antioxidant defense mechanisms of both the cell lines it could be really interesting to find the defense mechanisms of R3 cells that allow them to cope up with the stress induced by mtDNA depletion. Thus, these results might indicate the important role that Schwann cells play in complementing neurons providing essential metabolites and thereby helping them survive the deleterious effects such as mtDNA depletion, although this merits further investigation.

In our study we have also investigated the role of mtDNA depletion in affecting mitochondrial dynamics. Defective mitochondrial dynamics have been implicated in variety of neurodegenerative disorders including peripheral neurodegeneration. Previous studies have indicated that defective mitochondrial dynamics lead to mtDNA depletion (King et al., 1989) and our study has provided support for the notion that the vice versa could also be true. Our results indicate that chronic mtDNA depletion leads to depletion of mitofusin-1 expression in both the cell lines but the expression of mitofusin-2 was relatively unaltered. Confocal microscopic studies with DRG neurons have also strengthened the fact that the mitochondrial fusion is affected.

Conclusions

Our study has demonstrated that chronic mtDNA depletion in DRG neurons and Schwann cells induced morphological changes and alterations in the activities of various enzymes involved in oxidative metabolism and decreases in mitochondrial mass. Concurrently, the study also noted the role of mtDNA aberrations in inducing oxidative stress and impairing

mitochondrial fusion. The effect of chronic mtDNA depletion was found to be more pronounced in DRG neurons than that of Schwann cells. Thus, our results may have some pathophysiological implications in the peripheral neuropathy and its related disorders.

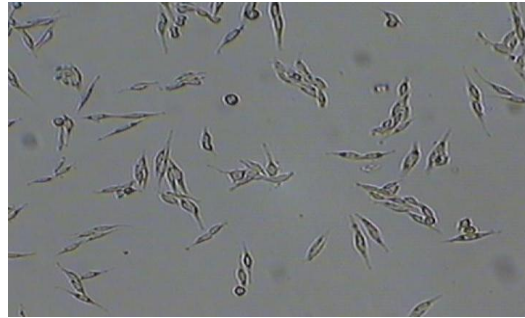
Acknowledgement

We whole-heartedly thank Dr. Ahmet Höke of Johns Hopkins University School of Medicine for his generous gift of dorsal root ganglion neurons.

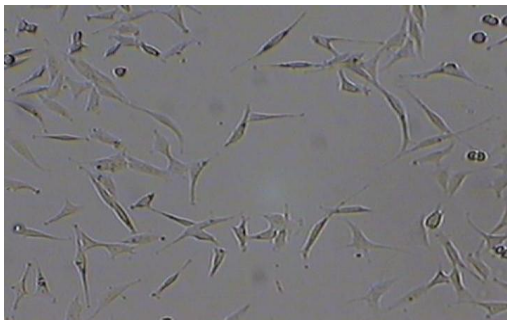
Figures



DRG CONTROL



R3 CONTROL



DRG TREATED



R3 TREATED

Figure 1. DRG neurons and Schwann cells and their respective ρ^0 cells viewed under light microscopy.

Images of control (i.e., untreated) and ρ^0 (i.e., treated with ethidium bromide for 4 weeks) cells were taken in bright field microscopy at 400x magnification. The ρ^0 cells appeared shrunken and smaller as compared to their respective controls.

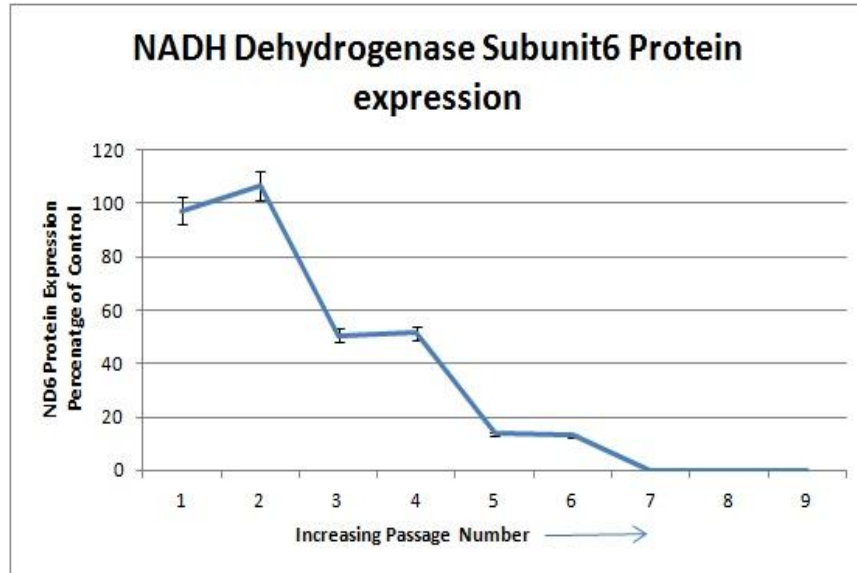


Figure 2. Expression pattern of ND6 in DRG neurons treated with ethidium bromide over four weeks.

Cells were harvested after every second passage and lysates were made. Western blot analysis was performed using those lysates and the optical densities of ND6 bands were normalized with respect to their corresponding β -actin bands and plotted as a percentage of the same ratio in the control (i.e., untreated cells); the ratio in the untreated cells (control) was taken as 100%. Values were mean \pm SEM of 3 determinations; two other experiments showed very similar results.

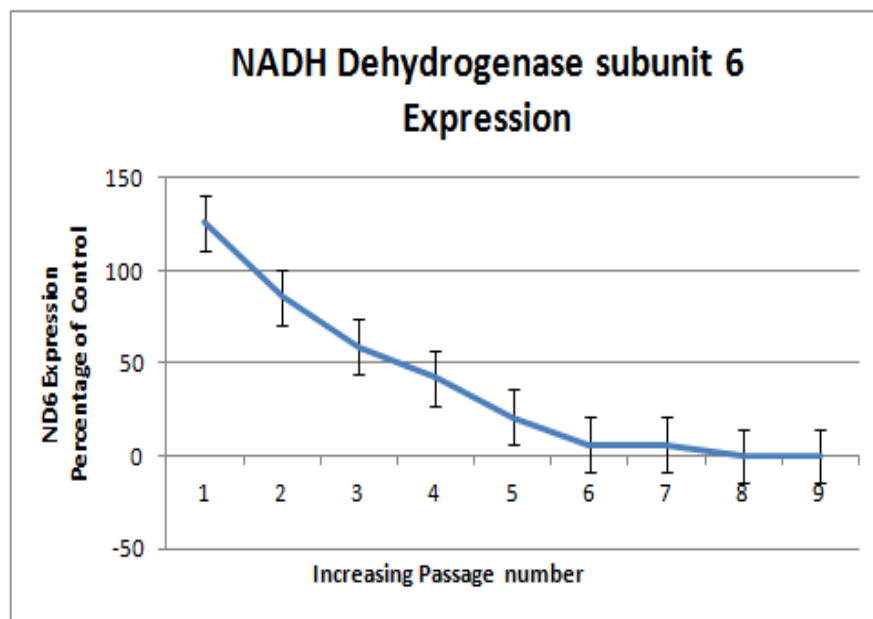


Figure 3. Expression pattern of ND6 in Schwann cells treated with ethidium bromide over four weeks.

Cells were harvested after every second passage and lysates were made. Western blot analysis was performed using those lysates and the optical densities of ND6 bands were normalized with respect to their corresponding β -actin bands and plotted as a percentage of the same ratio in the control (i.e., untreated cells); the ratio in the untreated cells (control) was taken as 100%. Values were mean \pm SEM of 3 determinations; two other experiments showed very similar results.

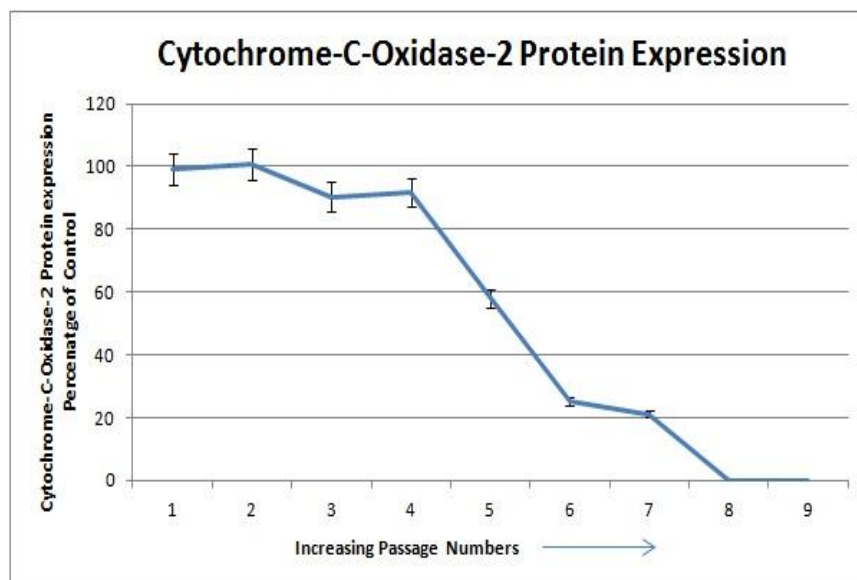


Figure 4. Expression pattern of cytochrome c oxidase subunit 2 in DRG neurons treated with ethidium bromide over four weeks.

Cells were harvested after every second passage and lysates were made. Western blot analysis was performed using those lysates and the optical densities of ND6 bands were normalized with respect to their corresponding β -actin bands and plotted as a percentage of the same ratio in the control (i.e., untreated cells); the ratio in the untreated cells (control) was taken as 100%. Values were mean \pm SEM of 3 determinations; two other experiments

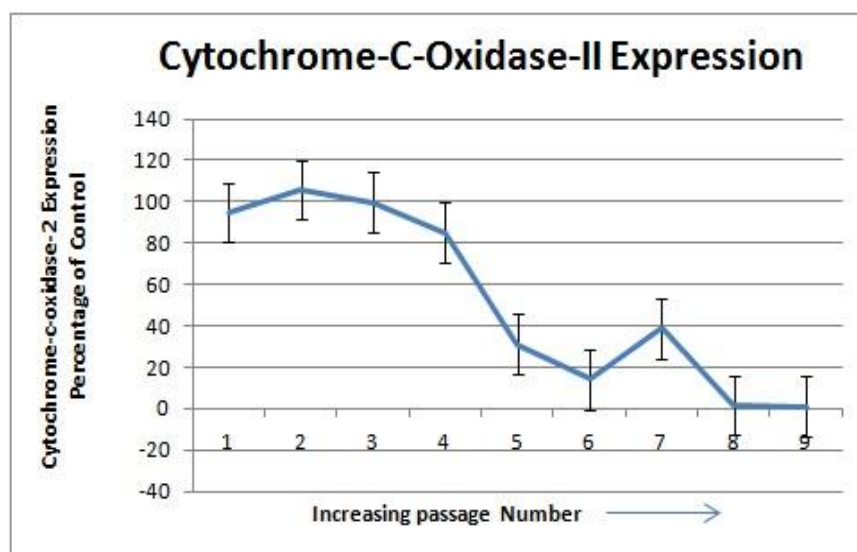


Figure 5. Expression pattern of cytochrome c oxidase subunit 2 in Schwann cells treated with ethidium bromide over four weeks.

Cells were harvested after every second passage and lysates were made. Western blot analysis was performed using those lysates and the optical densities of ND6 bands were normalized with respect to their corresponding β -actin bands and plotted as a percentage of the same ratio in the control (i.e., untreated cells); the ratio in the untreated cells (control) was taken as 100%. Values were mean \pm SEM of 3 determinations; two other experiments showed very similar results.

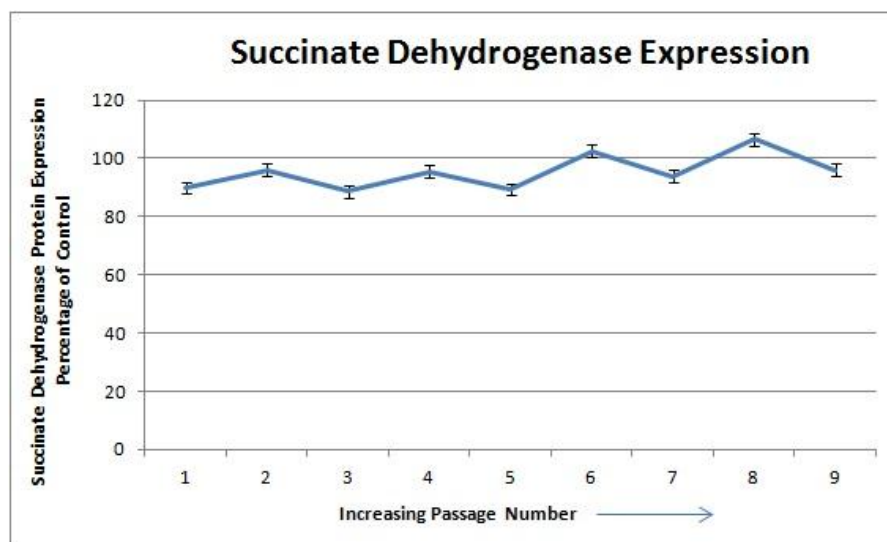


Figure 6. Expression pattern of Succinate Dehydrogenase in Schwann cells treated with ethidium bromide over four weeks.

Cells were harvested after every second passage and lysates were made. Western blot analysis was performed using those lysates and the optical densities of SDH bands were normalized with respect to their corresponding β -actin bands and plotted as a percentage of the same ratio in the control (i.e., untreated cells); the ratio in the untreated cells (control) was taken as 100%. Values were mean \pm SEM of 3 determinations; two other experiments showed very similar results.

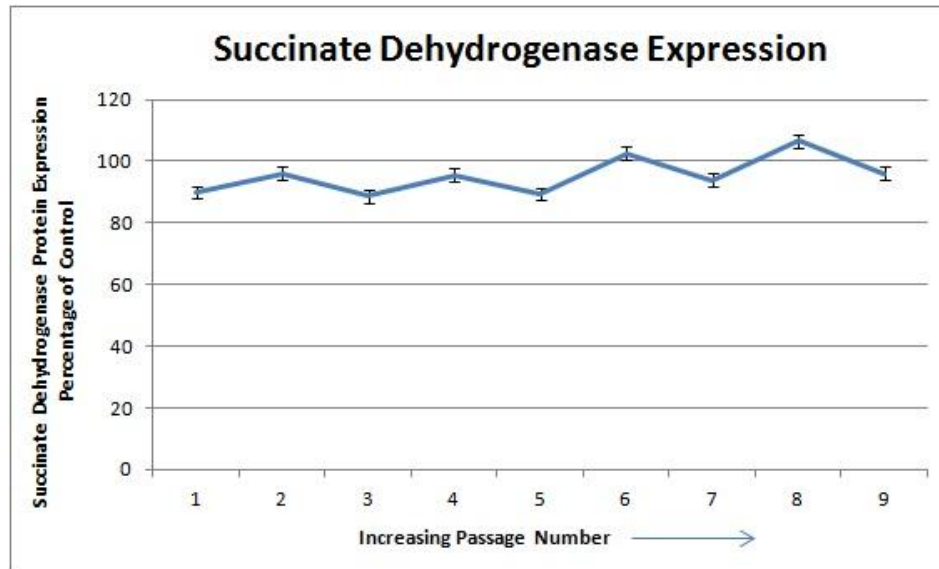


Figure 7. Expression pattern of Succinate dehydrogenase in DRG cells treated with ethidium bromide over four weeks.

Cells were harvested after every second passage and lysates were made. Western blot analysis was performed using those lysates and the optical densities of SDH bands were normalized with respect to their corresponding β -actin bands and plotted as a percentage of the same ratio in the control (i.e., untreated cells); the ratio in the untreated cells (control) was taken as 100%. Values were mean \pm SEM of 3 determinations; two other experiments showed very similar results.

Measurement of mitochondrial mass

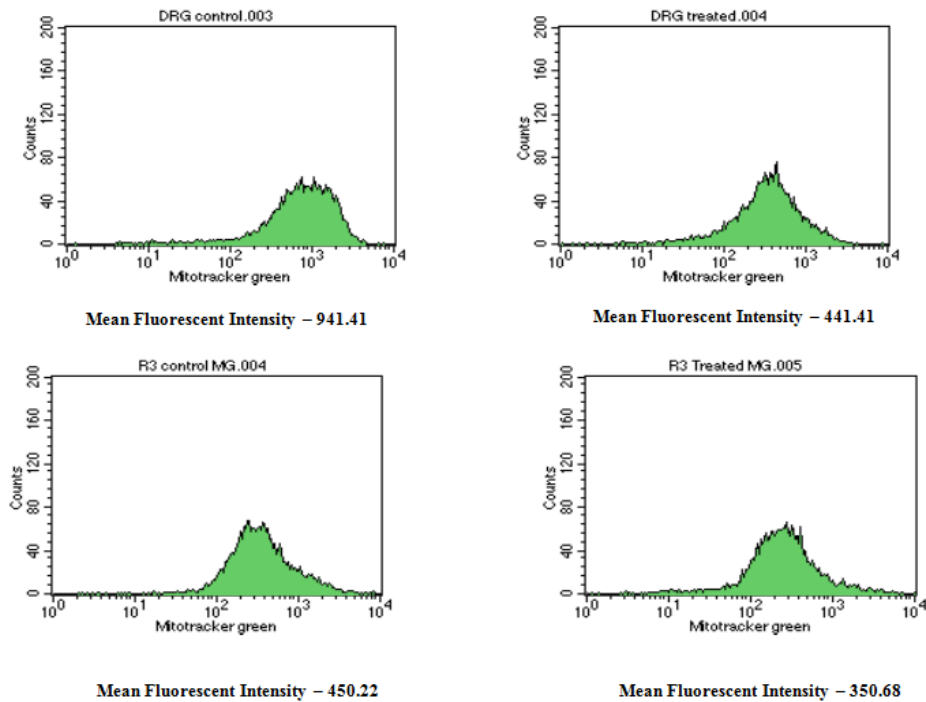


Figure 8. Effect of mtDNA deletion on mitochondrial mass in DRG neurons and Schwann cells.

DRG neurons and Schwann cells and their respective p^0 cells were harvested when they were at ~ 70% confluency and, then stained with 100mM Mitotracker Green. The mean fluorescence intensities in the stained cells were determined using a FACS-Calibur flow cytometer.

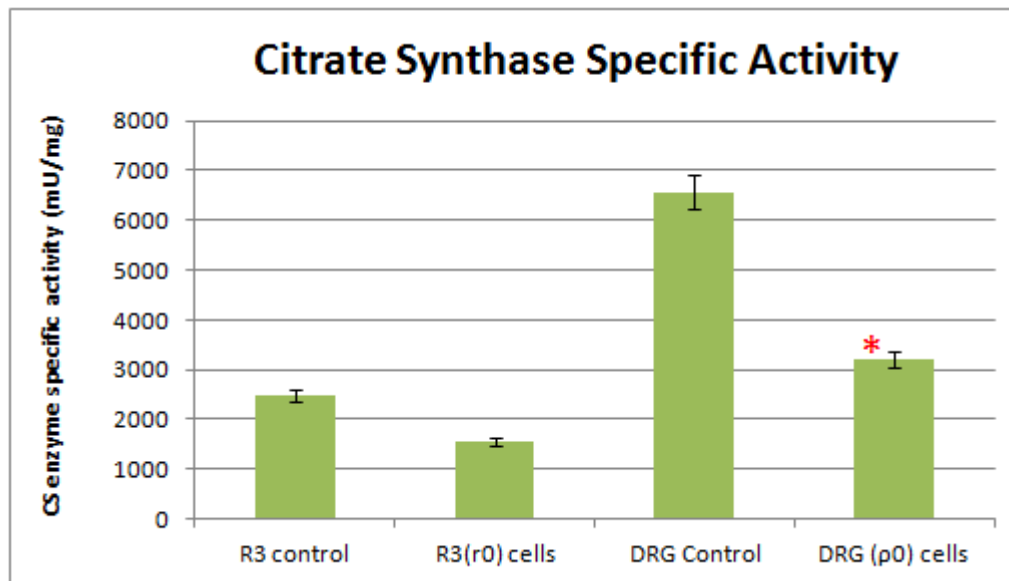


Figure 9. Citrate synthase activities in Schwann cells and DRG neurons and in their respective p^0 cells.

Enzyme activity of Citrate Synthase was measured using UV-Vis spectrophotometer and specific activity was calculated by normalizing with the protein content in the samples. Values are mean \pm SEM of 3 determinations; * $p < 0.05$ versus corresponding control value.

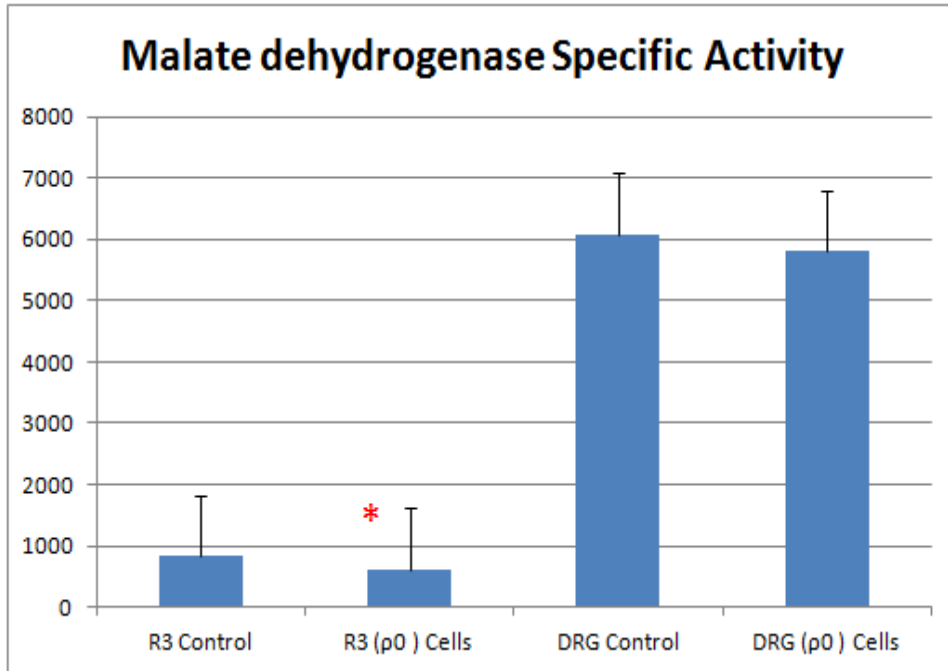


Figure 10. Malate dehydrogenase activities in Schwann cells and DRG neurons and in their respective ρ^0 cells.

Enzyme activity of MDH was measured using UV-Vis spectrophotometer and specific activity was calculated by normalizing with the protein content in the samples. Values are mean \pm SEM of 3 determinations; * $p < 0.05$ versus corresponding control value.

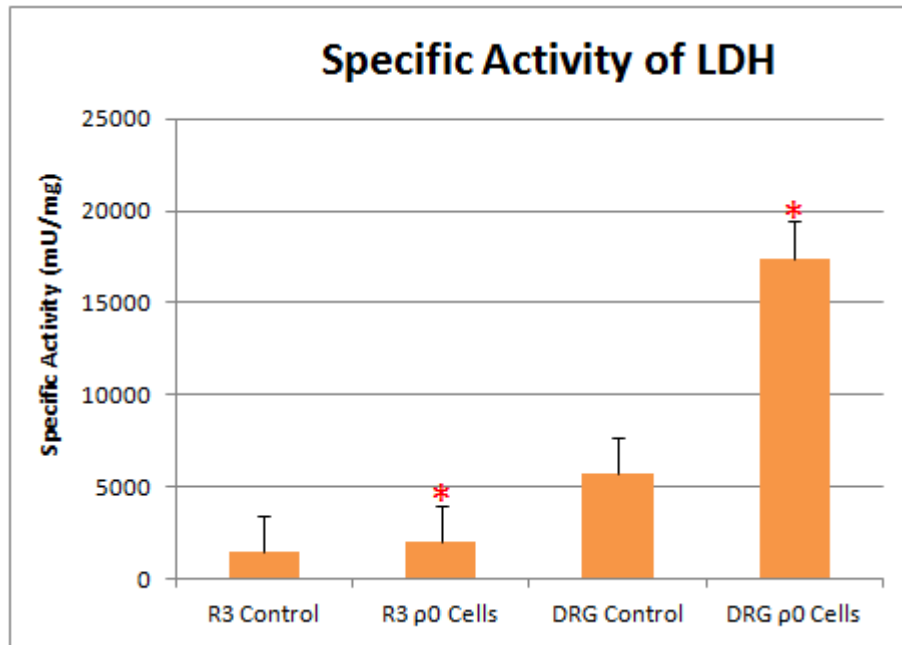


Figure 11. Lactate dehydrogenase activities in Schwann cells and DRG neurons and in their respective p⁰ cells.

Enzyme activity of LDH was measured using UV-Vis spectrophotometer and specific activity was calculated by normalizing with the protein content in the samples. Values are mean \pm SEM of 3 determinations; *p<0.05 versus corresponding control value.

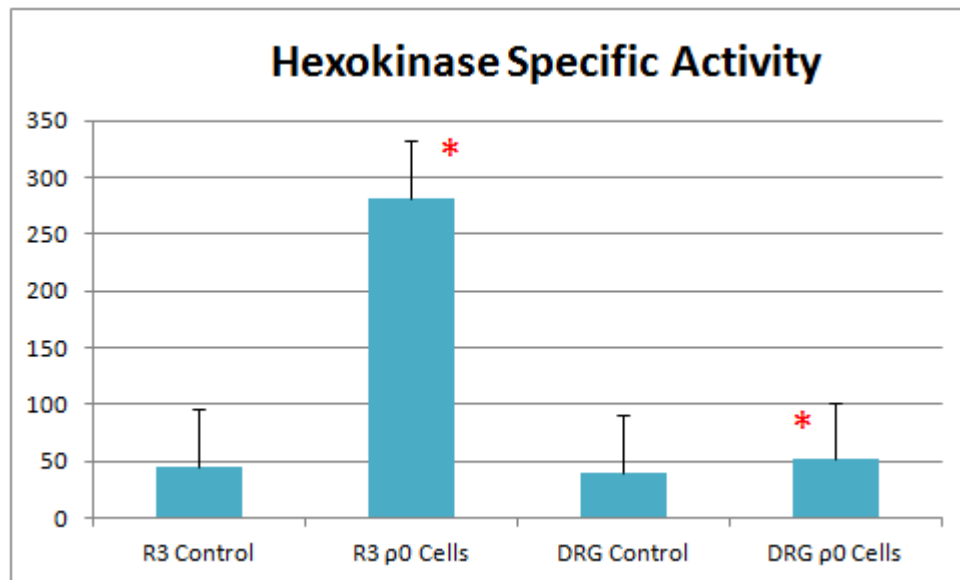


Figure 12. Hexokinase activities in Schwann cells and DRG neurons and in their respective ρ^0 cells.

Enzyme activity of Hexokinase was measured using UV-Vis spectrophotometer and specific activity was calculated by normalizing with the protein content in the samples. Values are mean \pm SEM of 3 determinations; * $p < 0.05$ versus corresponding control value.

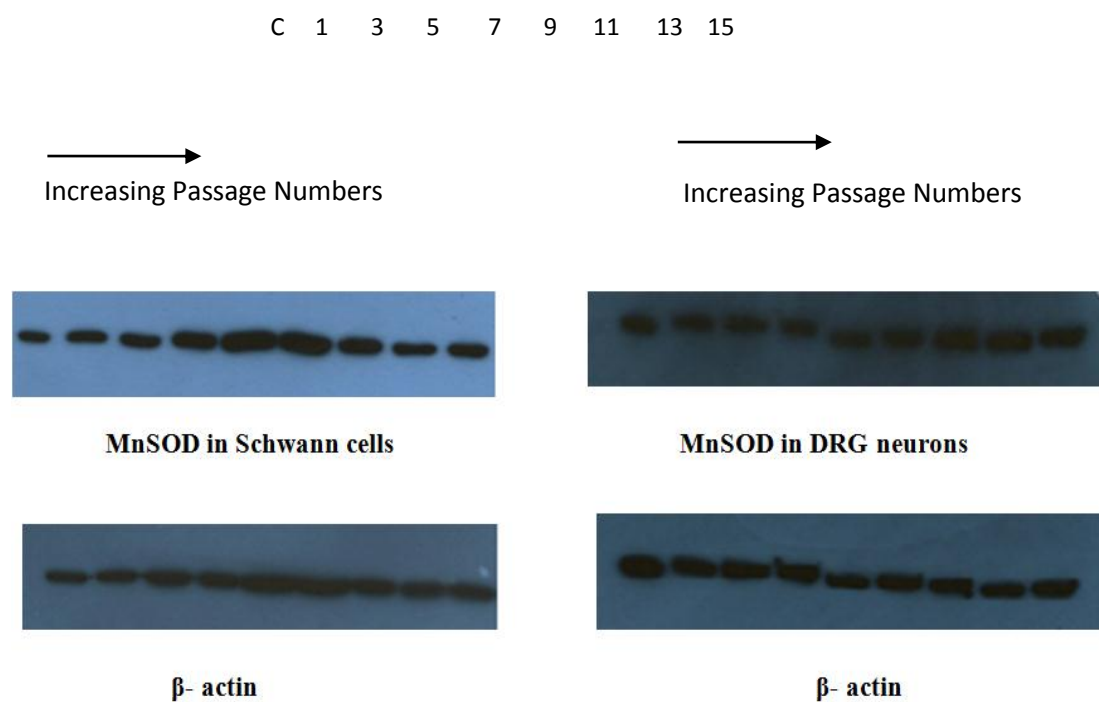


Figure 13. Expression pattern of MnSOD in Schwann cells and DRG neurons treated with ethidium bromide over four weeks.

Cells were harvested after every second passage and lysates were made. Western blot analysis was performed using those lysates.

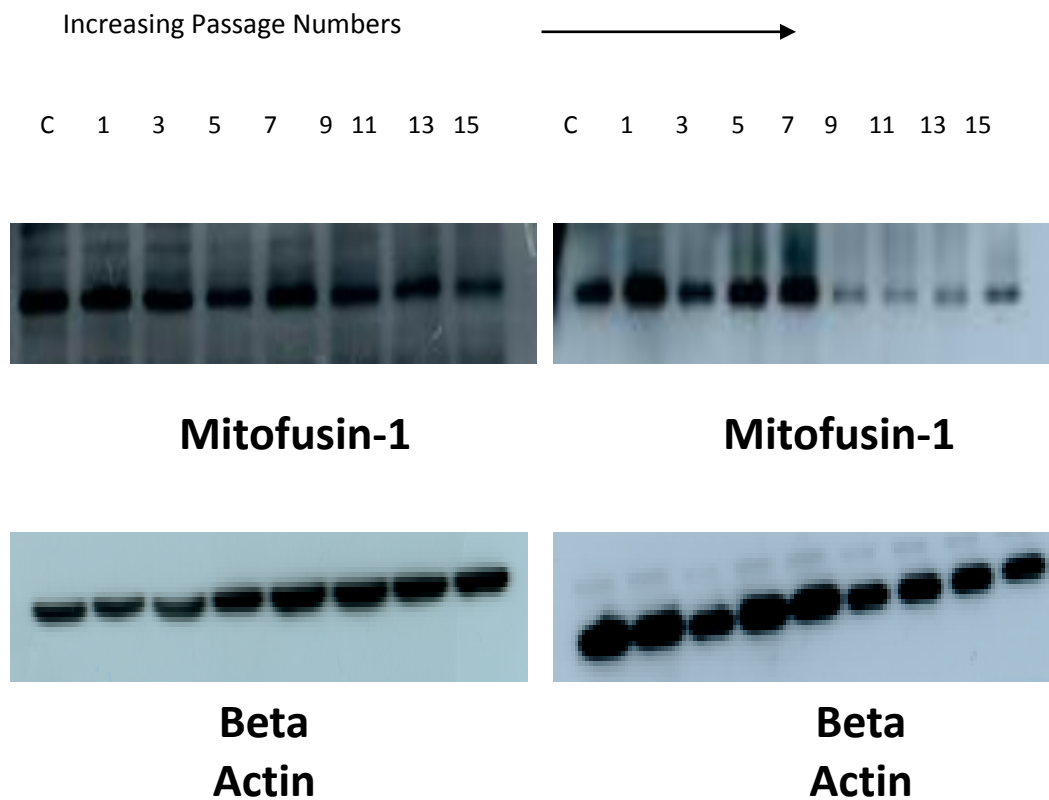


Figure 14 . Effect of mtDNA deletion on expression of Mitofusin-1 (Mfn-1) in DRG neurons and Schwann cells.

DRG neurons were treated with ethidium bromide over 15 weeks and their expression of Mfn-1 was determined by Western blot analysis.

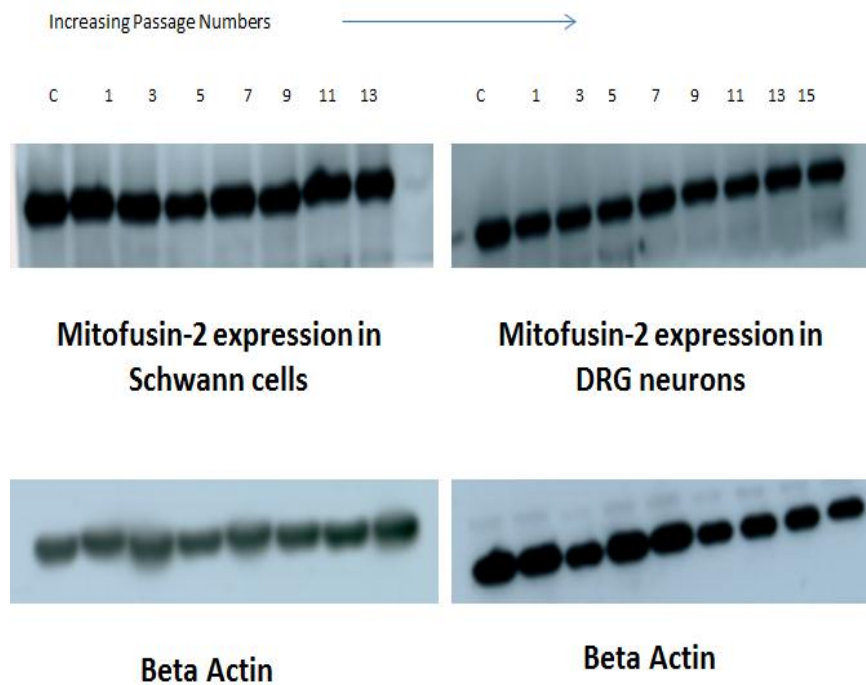
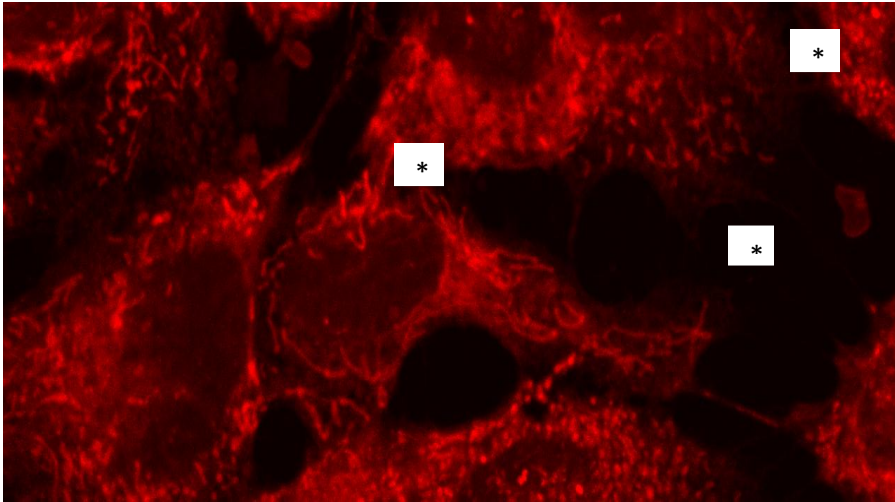


Figure 15. Effect of mtDNA deletion on expression of Mitofusin-2 (Mfn-2) in DRG neurons and Schwann cells.

DRG neurons were treated with ethidium bromide over 15 weeks and their expression of Mfn-2 was determined by Western blot analysis.

DRG Control



DRG ρ^0 cells

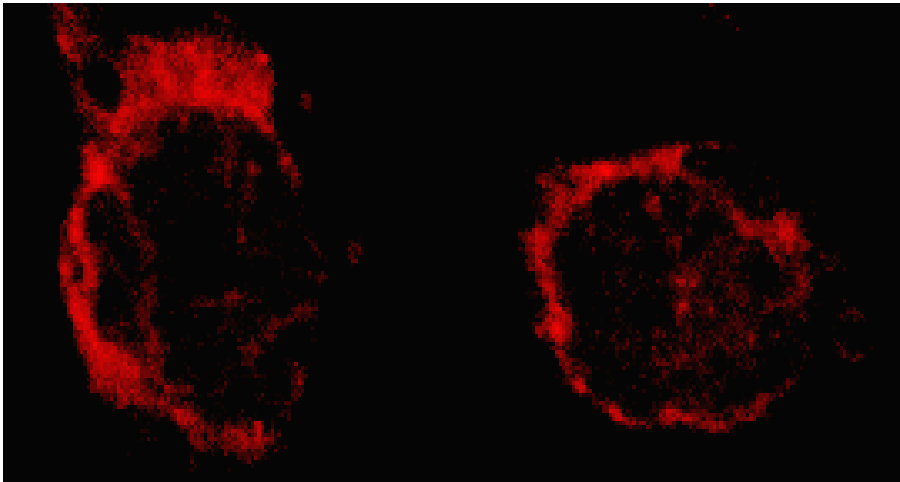


Figure 16. Effect of mtDNA deletion on mitochondrial dynamics in DRG neurons employing confocal microscopy.

DRG neurons and their ρ^0 cells were seeded on cover slips, fixed and stained with Mitotracker deep red. The stained cells were then viewed with an Olympus FV1000 confocal microscope and the fluorescence images of the cells were acquired employing the CCD camera and the Micromanager Acquisition software Magnification- 100X.

References

- Ayyasamy V, Owens KM, Desouki MM, Liang P, Bakin A, Thangaraj K, Buchsbaum DJ, LoBuglio AF, Singh KK (2011). Cellular model of warburg effect identifies tumor promoting function of UCP2 in breast cancer and its suppression by genipin. PLoS One, 6(9):71-79.
- Beal MF (2005). Mitochondria take center stage in aging and neurodegeneration. Ann Neurol. 58:495–505.
- Beal MF (2007). Mitochondria and neurodegeneration. Novartis Found Sym. 287:183–192.
- Bubber P, Haroutunian V, Fisch G, Blass JP, Gibson GE (2005). Mitochondrial abnormalities in Alzheimer brain: mechanistic implications. Ann Neurol. 57:695–703.
- Chacinska S, Koehler CM, Milenkovic, Lithgow DT, Pfanner N (2009). Importing mitochondrial proteins: machineries and mechanisms. Cell. 13(4):628–644.
- Chen W, Mi R, Haughey N, Oz M, Höke A (2007) immortalization and characterization of a nociceptive dorsal root ganglion sensory neuronal line. J Peripher Nerv Syst 12(2): 121-130.
- Clark JB, Lai JCK (1989) Glycolytic, tricarboxylic acid cycle and related enzymes in brain. In NeuroMethods, Vol. 11 (Boulton AA, Baker GB & Butterworth RF, eds.), pp. 233-281, Humana, Clifton, NJ.
- De Vivo DC, Hirano M, DiMauro S (1996). Mitochondrial disorders. In Handbook of Clinical Neurology, vol. 22 (H. W. Moser ed.), pp. 389–446, Elsevier, Amsterdam, NY.

DiMauro S, Hirano M, Bonilla E, De Vivo DC (1996). The mitochondrial disorders. In Principles of Child Neurology, vol. 4 (B. O. Berg ed.), pp. 1201–1232, McGraw-Hill, New York City, NY.

DiMauro S, Bonilla E (1997). Mitochondrial encephalomyopathies. In The molecular and genetic basis of neurological disease, vol.2 (R. N. Rosenberg, S. B. Prusiner, S. DiMauro and R. L. Barchi eds.), pp. 201–232, Butterworth-Heinemann, Boston, MA.

Gibson GE, Sheu KF, Blass JP (1998). Abnormalities of mitochondrial enzymes in Alzheimer's disease. J Neural Transm. 105:855–870.

Hughes JA (1994). Mitochondrial diseases. In Myology, 2nd ed. (A. G. Engel and C. Franzini-Armstrong eds.), pp. 1610–1660, McGraw-Hill, New York City, NY.

Isaac AO (2007). Mitochondrial DNA depletion alters energy metabolism, antioxidant systems, and intergenomic signaling: implications in neurodegeneration, toxicity to nucleoside analogue-based HIV therapy and mitochondrial myopathy. Ph.D. Dissertation, Idaho State University, Pocatello, ID.

Isaac AO, Dukhande VV, Lai JC (2007). Metabolic and antioxidant system alterations in an astrocytoma cell line challenged with mitochondrial DNA deletion. Neurochem Res. 32(11): 1906-1918.

Isaac AO, Kawikova I, Bothwell AL, Daniels CK, Lai J. C. (2006). Manganese treatment modulates the expression of peroxisome proliferator-activated receptors in astrocytoma and neuroblastoma cells. Neurochem Res. 31(11):1305-1316.

Kim JA, Wei Y, Sowers JR (2008). Role of mitochondrial dysfunction in insulin resistance. Circulation Research. 102(4):401–414.

King MP, Attardi G (1989). Human cells lacking mtDNA: repopulation with exogenous mitochondria by complementation. *Science* 246:500-503.

Liang Q, Dedon PC (2001). Cu(II)/H₂O₂-induced DNA damage is enhanced by packaging of DNA as a nucleosome. *Chem Res Toxicol.* 14(4):416-422.

Nunez ME, Noyes KT, Barton JK (2002). Oxidative charge transport through DNA in nucleosome core particles. *Chem Biol.* 9(4):403-415.

Pena A, Chavez E, Carabez A, De Gomez-Puyou MT (1977). The metabolic effects and uptake of ethidium bromide by rat liver mitochondria. *Arch Biochem Biophys.* 180(2):522-529.

Pendergrass W, Wolf N and Poot M (2004). Efficacy of MitoTracker GreenTM and CMXRosamine to measure changes in mitochondrial membrane potentials in living cells and tissues. *Cytometry.* 61A:162-169.

Rousset S, Alves-Guerra MC, Mozo J (2004). The biology of mitochondrial uncoupling proteins. *Diabetes.* 53(1):130–135.

Vaillant F, Loveland BE, Nagley P, Linnane AW (1991). Some biochemical properties of human lymphoblastoid Namalwa cells grown anaerobically. *Biochem Int.* 23(3):571-580.

CHAPTER 3

**Chronic mitochondrial DNA-deletion induces changes in heat shock proteins
and reactive oxygen species and alters mitochondrial dynamics: implications
in peripheral neuropathy**

Aishwarya Neti¹, Vinay K. Idikuda¹, Anurag K. Balaraju¹, Alfred O. Isaac², Alok Bhushan³ and
James C.K. Lai¹

¹Department of Biomedical & Pharmaceutical Sciences, College of Pharmacy, Division of Health Sciences and Biomedical Research Institute, Idaho State University, Pocatello, ID 83209, USA

²Department of Pharmaceutical Sciences and Technology, School of Health Sciences and Technology, Technical University of Kenya, Nairobi, Kenya

³Department of Pharmaceutical Sciences, Jefferson School of Pharmacy, Thomas Jefferson University, Philadelphia, PA 19107, USA

Abstract

Mitochondrial dysfunction resulting from mutations and/or deletion of mitochondrial DNA (mtDNA) has been implicated in many neurological/neurodegenerative diseases, including peripheral neuropathy. To investigate the effects of mtDNA depletion in peripheral neuropathy, we have developed cell models of mtDNA deletion employing dorsal root ganglion (DRG) neurons and Schwann cells: both are neural cell types in peripheral nervous system. This study was initiated to test the hypothesis that mtDNA depletion induces disruption of communications between the nuclear and the mitochondrial genomes. Our results reveal that chronic mtDNA depletion in DRG neurons led to decreases in their expression of both HSP 70 and HSP 90 and alterations of their mitochondrial dynamics. Our results also demonstrated changes in cellular metabolism and alterations in anti-oxidant system. Thus, our results may assume pathophysiological importance in peripheral neuropathy in particular and neurodegeneration in general.

Key words: mitochondrial DNA depletion, mitochondrial dynamics, HSPs, oxidative stress.

Introduction

Mitochondria serve critical functions in maintenance of energy supplies, thermo-regulation, syntheses of essential molecules such as phospholipids and heme and mediate multiple signaling pathways. Alteration in mitochondrial function is responsible for a range of age-related neurodegenerative disorders (Di Mauro et al., 2005). Mitochondria undergo constant fission and fusion events and form a reticular structure, essential for the maintenance of the normal functions of mitochondria (Fraizer et al., 2007). In fact, mitochondrial fission and fusion are important to fine-tune cellular processes such as calcium homeostasis and generation of ATP; thus, they play important roles in cell cycle progression, apoptosis etc. (Patergnani et al., 2011).

Mitochondrial fusion is mediated by a small number of highly conserved guanosine triphosphatases (GTPases), called the mitofusins (Mfn-1 and Mfn-2), which mediate the outer membrane fusion, and optic atrophy factor-1 (OPA-1) which mediates the inner membrane fusion (Chan., 2006). Mitochondrial fission is mediated by dynamin family of proteins called the dynamic related protein-1 (DRP-1) (Zhao et al., 2011). However, the activity of DRP-1 is dependent on several other proteins, called the mitochondrial fission apparatus, consisting of mitochondrial fission protein-1 (Fis-1), mitochondrial fission factor (MFF) and mitochondrial elongation factor-1 (Zhao et al., 2011). Several proteins that mediate the mitochondrial fusion and fission, such as the mitofusins (Mfn-1 and Mfn-2), regulate the mitochondria-endoplasmic reticulum connectivity (De Brito et al., 2008). Additionally, Mfn-2, a mediator of mitochondrial fusion, acts as a transcriptional co-activator of peroxisome proliferator activated receptor gamma co-activator 1 α (PGC 1 α), which mediates mitochondrial biogenesis (Zorzano, 2009).

Mitochondrial fission and fusion events play a vital role in mitophagy, a quality control program of the mitochondria (Tolkovsky, 2009). Mitophagy selectively eliminates the damaged and depolarized mitochondria by lysosomes (Tolkovsky, 2009). Fission helps in isolating the depolarized mitochondria and fusion prevents the reintegration of the mitochondria, thereby facilitating mitophagy (Tolkovsky, 2009). Evidently, mitochondrial dynamics are involved in a wide range of normal cellular functions and alterations or mutations in mitochondrial fission and fusion proteins result in very specific neurodegenerative disorders (Kijima, 2005). For example, mutations in Mfn2 causes Charcot-Marie-Tooth subtype 2A (CMT2A), a peripheral neuropathy characterized by muscle weakness and axonal degradation of sensory and motor neurons (Kijima, 2005). Mutations in Opa1 cause the most common form of optic atrophy, autosomal dominant optic atrophy (ADOA) (Alexander et al., 2007). Patients with ADOA exhibit progressive loss of vision and degeneration of the optic nerve and retinal ganglion cells. A dominant negative mutation in the human DRP1 gene resulted in elongated and tangled mitochondria concentrated at peri-nuclear region (Waterham et al., 2007). Moreover, mutations in the ganglioside-induced differentiation-associated protein-1 (GDAP1), which appears to be involved in mitochondrial fission, have been associated with CMT neuropathy type 4A (Baxter et al., 2000).

Apart from mitochondrial dynamics, mitochondria are also essential regulators of mitochondrial bioenergetics (Lai and Clark, 1989; Clark and Lai, 1989; Melov et al., 2000). The normal balance in the cellular homeostasis and mitochondrial bioenergetics is attained by generation and elimination of the reactive oxygen species and reactive nitrogen species (ROS and RNS) (Le Bras et al., 2005). Various exogenous and endogenous agents can induce the formation of ROS. Exogenous substances include UV radiation; X-rays, atmospheric pollutants

etc. while the major source of endogenous ROS production in mitochondria (Le Bras et al., 2005). Mitochondrial production of ROS is mainly due to electron leak during the process of respiration. The components of the electron transport chain (ETC) are located in the inner membrane of the mitochondria (Rigoulet et al., 2011). During respiration, electrons are transferred to molecular oxygen through the complexes I to IV of the respiratory chain to form water. This process takes place in parallel with pumping the protons across the inner mitochondrial membrane (Rigoulet et al., 2011). During this process, electron leak may occur at complex I or III to form a superoxide anion (Rigoulet et al., 2011). Other conditions such as post-translational modifications of the ETC complexes (e.g., complex I) can also lead to formation of ROS (Taylor et al., 2003). The acetylation of the complex I and II can also modulate the activity of the ETC and alter respiration and production of ROS (Taylor et al., 2003). However, the ROS must be maintained at an optimum range for normal cellular homeostasis (Liochev et al., 2005).

Many mitochondrial antioxidant systems are involved in regulating the production of ROS. The superoxide dismutase (SOD) family of enzymes catalyzes the conversion of superoxide anion to hydrogen peroxide (Liochev et al., 2005; Dhukande et al., 2006, 2009). The formed hydrogen peroxide is further reduced by the members of catalase family or glutathione peroxidase family (GPx) and peroxiredoxin family (Prx) (Dhukande et al., 2006, 2009; Rigoulet et al., 2011). The GPx family of enzymes relies on reduced glutathione (GSH) in the process of reducing hydrogen peroxide to water. During reduction of the peroxides, GSH is oxidized to GSSG, which is subsequently reduced back to GSH by glutathione reductase (GR) (Dhukande et al., 2006, 2009). Hence for the optimum activity of the GPx family of enzymes, it is important to maintain the intracellular levels of GSH (Rotruck, 1973; Dhukande et al., 2006, 2009).

Disruption of any of these enzymes systems can lead to an increase in the ROS levels, and consequently give rise to oxidative stress (Dhukande et al., 2006, 2009).

Mitochondrial oxidative stress is implicated in a variety of neurodegenerative disorders including Parkinson's disease (PD) (Schapira et al., 1999). Moreover, several metabolic enzymes containing iron-sulphur clusters (Fe-S), in particular aconitase and α -ketoglutarate dehydrogenase complex are sensitive to the intracellular concentrations of ROS (Tretter et al., 2005). Aconitase can be a sensitive target to ROS due to the presence of a single ligated iron atom. Increase in ROS can cause the Fe-S cluster instability due to oxidation of the single iron atom, leading to oxidative inactivation and loss of the enzyme activity (Vivar et al., 2000). In this pathophysiological context, it is relevant to note that loss of aconitase activity is associated with oxidative stress in several neurodegenerative diseases (Patel et al., 1996; Liang et al., 2004).

Heat shock proteins (HSPs) or molecular chaperones constitute another family of proteins that are known to play a vital role in minimizing oxidative stress (Kalmar et al., 2009). Apart from minimizing oxidative stress, HSPs play important mechanistic roles in protein folding and transport or targeting (Fox, 2012). It is also noteworthy that there is decreased expression of several classes of these chaperones in neurodegenerative disorders such as Parkinson's disease (PD) and Alzheimer's disease (AD) due to misfolding or degradation of these proteins (Selkoe, 2004).

Evidence has been accumulating implicating altered mitochondrial dynamics, enhanced oxidative stress, structural-functional alterations in heat shock proteins, and mitochondrial DNA (mtDNA) deletion or depletion in the central nervous system (CNS) in the etiology and pathophysiology of neurodegenerative diseases (Fox, 2012). However, similar

pathophysiological and/or pathogenetic mechanisms in neurodegenerative diseases in the peripheral nervous system (PNS) have not been fully elucidated. Previous studies from our laboratory demonstrated the expression of several metabolic and antioxidant enzymes were differentially altered in human astrocytoma U87 cells when challenged with mitochondrial DNA deletions (Isaac et al., 2007; Isaac, 2007). We have recently demonstrated dorsal root ganglion neurons (DRG) and Schwann cells can be productively employed to produce neural cell models in vitro whereby the mtDNA of neural cells can be chronically depleted (Jaiswal et al., 2010; Idikuda, 2013). This study was therefore initiated to test the hypothesis that chronic mtDNA deletion induces changes in mitochondrial dynamics and disruption of communication between mitochondrial and nuclear genomes employing DRG neurons in vitro as a PNS neural cell model.

Materials and Methods

Materials

Ethidium bromide was purchased from Sigma Aldrich (MO, USA), dialyzed FBS was purchased from Atlanta Biologicals (Norcross, GA), and Tween 20, sodium pyruvate, Dulbecco's Modified Eagle media (DMEM), L-glutamine, and phenol red were from Sigma (St. Louis, MO). SDH antibody was purchased from Santa-Cruz Biotechnology (Santa Cruz, CA). OPA-1, Drp-1, Synapsin-1, and HSP70 antibodies were purchased from Abcam (Cambridge, MA). ND6 and cytochrome-c-oxidase-2 antibodies were purchased from Molecular Probes (Eugene, OR). The chemiluminescence reagents and bicinchoninic protein assay (BCA) kit were obtained from Thermo Fisher (Waltham, MA) and autoradiography films were from Biomax (Rochester, NY). Protease inhibitor cocktail tablets were from Roche diagnostics (Mannheim,

Germany) and Mitotracker red dye was purchased from Invitrogen (Carlsbad, CA). Except otherwise stated, all other chemicals used were purchased from Sigma Aldrich (St. Louis, MO).

Cell Culture

Immortalized at dorsal root ganglion (DRG) neurons were a generous gift from Dr. Ahmet Hóke (Johns Hopkins University School of Medicine) (Chen et al., 2007). The cells were cultured in DMEM medium supplemented with 10% (v/v) dialyzed fetal bovine serum (Atlanta Biologicals, Norcross, GA), 100 µg/ml uridine, 1% (w/v) sodium pyruvate, 0.292 g/L L-glutamine, 1.5 g/L sodium bicarbonate, and 4.53 g/L glucose (Sigma Aldrich, St. Louis, MO). The cell lines were treated with 50 ng/ml ethidium bromide (Sigma Aldrich, St. Louis, MO) over a period of 15 weeks to deplete their mitochondrial DNA. The cells were allowed to grow to 70% confluent for all the experiments mentioned hereafter and maintained at 5% (v/v) carbon dioxide and at 37°C.

Western Blot Analysis

DRG neurons were seeded in a T-75 flask and were incubated until 70% confluent. To prepare lysates, cells were washed in ice-cold 1X phosphate-buffered saline (PBS) thrice and harvested by using the lysis buffer containing Tris, sodium chloride, glycerol, EDTA, protease inhibitor cocktail, phenylmethylsulfonyl fluoride (PMSF) and sodium orthovanadate. The washed cells were collected and homogenized by sonication. The sonicated samples were then centrifuged at ~15,000 g for 10 min at 4°C. The resultant supernatant was collected and to it was added 2 X Lammeli buffer. The samples were heated at 90°C for 5 minutes and stored at -80°C. The proteins in the samples so prepared were separated by sodium dodecyl sulfate-polyacrylamide gel electrophoresis (SDS-PAGE) using 10% (w/v) gels. The separated proteins

were then transferred onto a polyvinylidene difluoride (PVDF) membrane and were blocked by using 5% (w/v) milk powder solution for an hour at room temperature. These blots were then washed with Tris-buffered saline (TBS) and incubated with the desired primary antibody overnight. The blots were then washed using TBS and incubated with HRP-conjugated secondary antibody for an hour and developed using chemiluminescence.

Confocal Microscopy

DRG neurons were cultured in DMEM medium containing ethidium bromide to generate cells devoid of mitochondrial DNA as described above. They were harvested and plated for confocal microscopy in a 6-well plate and the cells were then allowed to grow on a microscopic slide sterilized with ethanol. After the cells had attached to the slide, they were incubated with 500 nm Mitotracker deep red for 40 minutes at 37°C for the dye to enter the cells and stain the cells' mitochondria. Then the excess dye was removed and the slides were washed thrice with PBS. The washed cells were then fixed with 4% paraformaldehyde for 20 minutes. The cells were again washed with PBS. Subsequently, coverslips were mounted onto the glass slides using anti-fade reagent. Images of stained cells were acquired using the Olympus FV1000 confocal microscope a 60x oil-immersion objective and at 1024 x 1024 resolution. Confocal Z-stacks were acquired over 30 minutes and the photomicrographs were chosen at an optimum z-step.

BCA Protein Assay

Equal numbers of cells were plated in T-75 flasks and cells devoid of mitochondrial DNA were generated by treating them with ethidium bromide as described above. When they were ~70% confluent, the cells were harvested and lysate was prepared using lysis buffer as described above. Then the sonicated cell lysate was centrifuged at ~15,000 g for 10 min at 4° C and the

resultant supernatant fraction was collected as described above and stored at -70° C until it was employed for experiments. The protein content of the supernatant fractions was determined employing the BCA protein Assay kit (Fischer Thermo Scientific, Waltham, MA) as described previously (Dhukande et al., 2013).

ROS Assay

A rapid and sensitive luminescent ROS assay was used to determine the production of reactive oxygen species (ROS) by the cultured DRG neurons. The control cells and the ethidium bromide-treated cells (i.e., cells devoid of mitochondrial DNA) were plated in the 6-well plates and were allowed to attach to the plate. Then the cell-permeant 2', 7'-dichlorodihydrofluorescein diacetate (H₂DCFDA) was dissolved in DMSO to prepare the stock solution. The stock solution was diluted to the required concentration using PBS. Dye solution (200 µl) was added to each well of the 6-well plates and the plates were incubated at 37° C for 30, 40 or 90 minutes in the dark. The fluorescence of each well was then recorded at 517 nm (Excitation/Emission: ~492–495/517–527 nm). After their fluorescence was recorded, the BCA protein assay was employed to determine protein content of samples.

GSH Assay

GSH content in the cells was determined as described previously by Dhukande et al. (2007). Briefly, DRG neurons were cultured in T-75 flasks and harvested after they reached 75% confluency by using a homogenizing buffer containing salicylic acid (4.31% (w/v)) and 0.25 mM EDTA. The total GSH in the cells was then determined by monitoring the chemical reaction between GSH and Ellmann's reagent at 412 nm.

Results

Maintenance of DRG neurons without mitochondrial DNA in culture

We (Isaac, 2007; Isaac et al., 2007; Idikuda, 2013) and others (King and Attardi, 1989) have demonstrated that cells chronically treated with a low concentration of ethidium bromide (EB) to deplete their mtDNA require the supplement of uridine in the DMEM used to maintain them in culture. Thus, to confirm that DRG neurons depleted of their mtDNA could not grow without the uridine supplement, we monitored by light microscopy the growth of DRG neurons that had been chronically treated with EB in DMEM medium with or without uridine supplement (data not shown). We found that DRG neurons chronically treated with EB stopped growing in the medium without uridine supplement, thereby confirming that those neurons were depleted of their mtDNA (King and Attardi, 1989; Isaac, 2007; Isaac et al., 2007; Idikuda, 2013) while the same neurons cultured in the medium with urine supplement continued to grow and to thrive.

Confirmation of DRG neurons chronically treated with EB exhibited depletion of their mitochondrial DNA (mtDNA)

In addition to employing the urine requirement as a criterion of confirming that DRG neurons chronically treated with EB exhibited mtDNA deletion, we also employed western blot analysis to confirm the extent of mtDNA depletion induced by EB-treatment in DRG neurons by monitoring the expression of mtDNA-encoded polypeptides such as NADH dehydrogenase subunit 6 (ND6, a protein subunit of complex I) (Isaac, 2007; Isaac et al., 2007; Idikuda, 2013). Our finding (Fig. 1) that chronic exposure of DRG neurons to EB induced time-related decreases in expression of ND6 demonstrated that the DRG neurons cultured in the presence of EB

progressively lost their mtDNA. Furthermore, as succinate dehydrogenase (SDH), a component of complex II, is a complex entirely encoded by nuclear DNA, our observation (Fig. 2) that the protein expression of SDH was typically not affected by chronic exposure of DRG neurons to EB suggested that our EB treatment did not apparently affect nuclear DNA (Isaac, 2007; Isaac et al., 2007; Idikuda, 2013).

We also found that compatible to what we had previously noted in U87 cells (another neural cell type) chronically depleted of their mtDNA (Isaac, 2007; Isaac et al., 2007), DRG neurons chronically depleted of their mtDNA also appeared to be smaller in size compared to control DRG neurons not treated with EB (Fig. 3).

Chronic mtDNA deletion induced differential changes in expression of heat shock proteins

Because heat shock proteins play important roles in regulating oxidative stress and in protein folding and protein transport/targeting (Kalmar et al., 2009; Fox, 2012), we investigated the hypothesis that chronic deletion of mtDNA induces disruption of communication between the mitochondrial and nuclear genomes by altering structure and function of heat shock proteins. Consistent with our hypothesis, our results indicate that chronic exposure of DRG neurons to EB induced time-related decreases in their expression of HSP70 (Fig. 4) but transient increases (especially in passage numbers 16 through 19) followed by more sustained decreases (in passage numbers 21 through 25) in their expression of HSP90 (Fig. 5), as determined by Western blot analysis. Furthermore, our findings (Figs. 4 and 5) also suggested that, as the EB-treatment progressively deleted mtDNA from the DRG neurons, the communication between the mitochondrial and the nuclear genomes was disrupted.

Chronic deletion of mtDNA in DRG neurons led to differential alterations in expression of OPA-1 and DRP-1

Employing confocal microscopy, we have recent evidence in support of the hypothesis that chronic deletion of mtDNA in DRG neurons leads to alterations of their mitochondrial dynamics (Idikuda, 2013; also see Chapter 2 above). To investigate this hypothesis further, we examined the effects of chronic treatment of DRG neurons with ethidium bromide (EB) on their expression of optic atrophy factor-1 (OPA-1), a key protein that governs the inner membrane fusion of mitochondria, and dynamic related protein-1 (DRP-1), a member of the dynamin family of proteins that mediate mitochondrial fission. Our findings employing Western blot analysis indicated that in DRG neurons chronically treated with EB to deplete their mtDNA (Fig. 1), their expression of OPA-1 was decreased (Fig. 6) but their expression of DRP-1 was increased (Fig. 7) compared to those in control (i.e., DRG neurons not treated with EB). Thus, our findings (Figs. 6 and 7) strongly suggests that in DRG neurons chronically depleted of their mtDNA, their mitochondrial dynamic equilibrium between fusion (i.e., decreased fusion) and fission (i.e., increased fission) was shifted in favor of or towards fission.

Chronic exposure of DRG neurons to ethidium bromide (EB) induced time-related decreases in their expression of aconitase

Evidence is accumulating that in cells whose mtDNA is deleted, their metabolism alters and adapts for survival (King and Attardi, 1989; Isaac, 2007; Isaac et al., 2007; Idikuda, 2013). We therefore investigated this possibility further by examining the expression of aconitase (a key enzyme in the tricarboxylic acid (TCA) cycle) in DRG neurons that had been chronically deleted of their mtDNA by treatment with EB. Our results based on Western blot analysis (Fig. 8)

demonstrated that chronic treatment of DRG neurons with EB induced time-related decreases (especially in passage numbers 20 through 25 when their mtDNA were deleted (Fig. 1)) in their expression of aconitase, a protein encoded by nuclear DNA but destined for mitochondria. Thus, this finding suggested that chronic mtDNA deletion in DRG neurons induces decreases in TCA cycle metabolism and disruption of intergenomic communication (Isaac, 2007; Isaac et al., 2007; Idikuda, 2013).

Chronic exposure of DRG neurons to ethidium bromide (EB) induced decreased expression of synapsin-1

Synapsin-1 is a phospho-protein highly enriched in axons and nerve terminals, especially in the synaptic vesicles and its expression is known to be altered in nerve degeneration and regeneration (Roshal et al., 1995). Because DRG neurons chronically depleted of their mtDNA via chronic treatment with EB are significantly smaller than control DRG neurons and exhibit noticeable morphological changes (Fig. 3), we investigated the possibility that EB-treatment may induce altered expression of synapsin-1 in DRG neurons. Our results from Western blot analysis (Fig. 10) are consistent with this hypothesis and suggested the decreased expression of synapsin-1 may be functional relevant and pathophysiologically important in DRG neurons devoid of their mtDNA.

In this context, it is noteworthy that when “normal” DRG neurons were treated with forskolin, an agent that induces morphological and functional differentiation in DRG neurons (Chen et al. 2007), the forskolin-treated DRG neurons showed many more processes and apparent cell-to-cell connectivity (compare Fig. 9 with Fig. 3). By contrast, when DRG neurons that had been depleted of their mtDNA were then treated with forskolin in a similar manner, they

did not form as many processes nor did they show the kind of cell-to-cell connectivity noted in “normal” DRG neurons treated with forskolin (Fig. 9) suggesting that the DRG neurons devoid of mtDNA were less responsive to the effect of forskolin.

Chronic mtDNA deletion in DRG neurons induced increases in their production of reactive oxygen species (ROS)

Mitochondria constitute the major site of production of ROS. Because HSPs have a protective role in regulating oxidative stress (see above) and we found chronic mtDNA deletion induced decreases in expression of HSP70 (Fig. 4) and HSP90 (Fig. 5), we tested the hypothesis that DRG neurons devoid of mtDNA produces more ROS compared to “normal” DRG neurons. Our finding that DRG neurons devoid of mtDNA generally produced more ROS than “normal” DRG neurons (Fig. 11) is consistent with this hypothesis.

Chronic mtDNA deletion induced an increase in GSH in DRG neurons

Because DRG neurons devoid of mtDNA showed increased production of ROS compared to “normal” DRG neurons (Fig. 11), we were interested to determine if the glutathione (GSH, a major endogenously produced antioxidant) content of the DRG neurons devoid of mtDNA was affected by their increased ROS production. Our results indicated that the GSH content of DRG neurons devoid of mtDNA was generally higher than those in “normal” DRG neurons (Fig. 12), suggesting that the DRG neurons devoid of mtDNA were attempting to compensate for their increased ROS production by also elevating their GSH content.

Discussion

Employing an in vitro model of DRG neurons chronically deleted of their mtDNA, this study is the first to demonstrate that chronic deletion of mtDNA in DRG neurons induces (i) differential changes in their expression of heat shock proteins, (ii) changes in their mitochondrial dynamics, which may be mediated, at least in part, through altering their expression of OPA-1 and DRP-1, (iii) increases in their ROS production and in their GSH content, and (iv) a decreased in their expression of synapsin-1.

Chronic mtDNA deletion in DRG neurons induced differential changes in their expression of heat shock proteins

Heat shock proteins or molecular chaperones are known to play a vital role in minimizing oxidative stress (Kalmar et al., 2009) in addition to their established mechanistic roles in protein folding, transport, and targeting (Fox, 2012). It is also noteworthy that there is decreased expression of several classes of these chaperones in neurodegenerative disorders such as Parkinson's disease (PD) and Alzheimer's disease (AD) due to misfolding or degradation of these proteins (Selkoe, 2004). Mitochondrial DNA depletion induces opening of pores in the mitochondrial membrane to release cytochrome c and AIF (apoptosis-inducing factor) into the cytosol, which in turn, leads to the activation of caspases, which then cleave several proteins that execute cell death. Proteins that play a major role in this process include p53, Bcl-2, Bax and Bad (Liu et al., 2004). However, whether this mtDNA-induced apoptotic mechanism occurs in neurons, especially neurons from the peripheral nervous system (PNS) have not been elucidated.

While mutations in the fission or fusion genes and alteration in the expression of mitochondrial proteins are pathophysiologically and/or pathogenically important in neurodegeneration, especially in PD and AD (Luo et al., 2010), the effects of mtDNA deletion

on HSP structure and function have not been elucidated. We have therefore investigated these effects in our DRG neuron cell model of neural cells in the PNS (Jaiswal et al., 2010; Idikuda, 2013). In this study, we found that chronic deletion of mtDNA induces time-related alterations in the expression of HSP70 and HSP90 (Figs. 4 and 5).

HSP70 interacts with regulators of many signal transduction pathways controlling cell homeostasis, proliferation, differentiation and cell death (Mayer and Bukau, 2005). Because HSP70 is encoded by nuclear DNA (nDNA), our finding of decreased expression of HSP70 in DRG neurons depleted of their mtDNA may suggest that the intergenomic communication between mtDNA and nDNA was disrupted in the DRG neurons devoid of mtDNA. Thus, the decreased expression of HSP70 in these neurons may compromise their normal functions such as proliferation, differentiation and cell death (Mayer and Bukau, 2005) are concerned. Indeed, our published (Isaac, 2007; Isaac et al., 2007; Idikuda, 2013) unpublished observations indicating that neural cells depleted of their mtDNA generally proliferate slower than counterparts with intact mtDNA. Thus, we may tentatively conclude that the decreased HSP70 expression in DRG neurons devoid of mtDNA may compromise their ability to proliferate. Evidently, further studies are needed to clarify this interesting mechanistic issue.

HSP90 is known to interact with many client proteins: the best characterized client proteins of HSP90 include steroid hormone receptors, protein kinases, and many transcription factors (Eckl and Richter, 2013). Moreover, in eukaryotic cells, expression of HSP90 is enhanced when they are stressed: indeed, that was how HSP90 was initially discovered as a heat shock protein (Eckl and Richter, 2013). Thus, our finding that the expression of HSP90 showed an initially up-regulation in DRG neurons as they were chronically deleted of their mtDNA may be attributed to the possibility that its initial up-regulation reflected DRG neurons' reaction and

adaptive response (e.g., via its interaction with Akt, a phospho-protein which regulates cell survival and proliferation (Eckl and Richter, 2013)) to oxidative stress induced by mtDNA deletion.

In primary cultures of dorsal root ganglion neurons chronically exposed to hyperglycemia (45 mM glucose in their culture medium), which is an in vitro model suitable for investigating pathophysiological mechanisms underlying diabetic peripheral neuropathy (DPN), inhibition of HSP90 by the selective inhibitor KU-32 induces decreases in mitochondrial superoxide levels and results in improvement of protein targeting to mitochondria (Zhang et al., 2012). Thus, our finding that chronic mtDNA deletion in DRG neurons ultimately led to sustained decreases in their HSP90 expression may reflect similar adaptive responses to combat or diminish the effects of oxidative stress because lowering the functional capacity of HSP90 appears to improve their ability to cope with or combat oxidative stress (Zhang et al., 2012). Nevertheless, although interesting and of pathophysiological relevance, these fluctuations in HSP90 expression in DRG neurons induced by chronic mtDNA deletion require further elucidation.

Chronic mtDNA deletion in DRG neurons induced changes in mitochondrial dynamics and differential expression of OPA-1 and DRP-1s

After DRG neurons were stained with Mitotracker deep red and when examined under the confocal microscope (see Chapter 2 for details), DRG neurons not devoid of their mtDNA (i.e., control DRG neurons) showed many fused mitochondria linked into strands-like structures both surrounding the nucleus and elsewhere in the cytoplasm as well as some single non-fused mitochondria: this finding suggested that in those cells the balance of mitochondrial dynamics in favor of fusion. By contrast, DRG neurons chronically depleted of their mtDNA exhibited

morphologies significantly different from those of control DRG neurons (see Chapter 2 for details). DRG neurons devoid of mtDNA contained far more fragmented or unfused mitochondria and very few fused mitochondria, linked into strands-like structures, strongly suggesting that the balance in their mitochondrial dynamics had been altered and shifted toward or in favor of fission. These observations prompted us to further investigate some of the molecular mechanisms underlying the mtDNA depletion-induced changes in mitochondrial dynamics in DRG neurons by examining their expression of OPA-1 and DRP-1 (Figs. 6 and 7).

OPA-1 is an essential protein required for inner membrane fusion of mitochondria (Chan, 2006). We found there was a decrease in OPA-1 expression in DRG neurons devoid of mitochondrial DNA when compared to that in control DRG neurons (Fig. 6), suggesting that mitochondrial fusion in DRG neurons depleted of their mtDNA was likely to be decreased. On the other hand, in DRG neurons depleted of their mtDNA, we noted their expression of DRP-1 was significantly increased compared to that in the control DRG neurons (Fig. 7): this observation suggested that mitochondrial fission was enhanced in DRG neurons depleted of their mtDNA because DRP-1 is an essential protein that mediates mitochondrial fission (Chan, 2006). Thus, our finding of decreased OPA-1 expression but increased DRP-1 expression in DRG neurons depleted of their mtDNA (Figs. 6 and 7) provide a molecular mechanism that could account for our conclusion that mtDNA depletion induces a change in the equilibrium of mitochondrial dynamics in favor of fission based on morphological studies employing confocal microscopy (see Chapter 2 for details).

Peripheral neuropathy is common and a predominant manifestation in many of the mitochondrial disorders (Pareyson, 2013). Thus, our finding that chronic mtDNA deletion induces changes in mitochondrial dynamics in favor of mitochondrial fission in DRG neurons

strongly suggests that mtDNA defect may be one important pathophysiological mechanism underlying peripheral neuropathy. Moreover, our finding may also assume pathophysiological importance in neurodegeneration such as in Alzheimer's disease (AD) and in Parkinson's disease (PD) because changes in mitochondrial dynamics are found in several neurodegenerative diseases including AD and PD, implicating dysregulation of DRP-1 as a key mechanism (Cho et al., 2013).

Chronic mtDNA deletion in DRG neurons induced increases in their production of reactive oxygen species (ROS)

As stated above, increase in the production of ROS is involved in pathophysiology of many neurodegenerative disorders such as PD and AD (Uttara et al., 2009). We also found DRG neurons depleted of their mtDNA exhibited an increase in their production of ROS (Fig. 11). This increase in their ROS production could be attributed, in part, to their decreases in manganese superoxide dismutase expression as their mtDNA was deleted (see Chapter 2 for details). Thus, DRG neurons depleted of their mtDNA also exhibit pathophysiological characteristics similar to those in neurons in neurodegenerative disorder such as PD and AD (Uttara et al., 2009).

Chronic mtDNA deletion induced an increase in GSH in DRG neurons

Because we found chronic mtDNA deletion in DRG neurons induced an enhancement in their ROS production (Fig. 11), we were curious to determine if their glutathione (GSH) content might reflect how they were coping with the enhanced ROS production. Our finding that DRG neurons depleted of their mtDNA had higher GSH levels than those in control DRG neurons (Fig. 12) suggests that the chronic mtDNA deletion elicited a compensatory mechanism in those

neurons in that their steady-state GSH levels were elevated. Even though their GSH levels were increased (Fig. 12), such increased GSH was not adequate to off-set the increases in ROS production induced by mtDNA deletion in those neurons, with the net outcome that such neurons were still under oxidative stress. As already alluded to above, this continued presence of oxidative stress was associated with alteration of mitochondrial dynamics in favor of mitochondrial fission and disruption of the normal communication between the nuclear and mitochondrial genomes.

Chronic exposure of DRG neurons to ethidium bromide (EB) induced decreases in their expression of synapsin-1

Synapsin family of proteins are a class of proteins that mediate the neurotransmitter release in the synapses (Kugler et al., 2003) and synapsin-1 is a marker of synaptic integrity and therefore neuronal integrity (Ziehn et al., 2012). We therefore investigated the possibility that chronic mtDNA deletion may also induce changes in synaptic plasticity and integrity in DRG neurons by examining the expression of synapsin-1 in DRG neurons with and without mtDNA depletion (Fig. 10). Our finding that chronic deletion in mtDNA induces decreases in synapsin-1 expression suggests that depletion of mtDNA in DRG neurons also induces changes in their synaptic plasticity and function and as such mimics cellular pathologies detected in neurodegeneration (Ziehn et al., 2012). Nevertheless, this interesting observation awaits further mechanistic clarification.

Conclusions

Taken together, the results of this study indicate that chronic deletion of mtDNA in DRG neurons induced (i) changes in their oxidative metabolism concomitant with disruption of their

mitochondrial dynamics through the down-regulation of OPA-1 but up-regulation of DRP-1, (ii) differential alterations (both initial up-regulation and subsequent more sustained down-regulation) of their HSP90 expression but down-regulation of their HSP70 expression, (iii) continued oxidative stress via enhancing their ROS production even in the presence of apparent compensatory elevation of their GSH levels, and (iv) disturbance of their synaptic plasticity and integrity by lowering their expression of synapsin-1. Thus, our findings may assume pathophysiological importance not only in peripheral neuropathy in particular but neurodegeneration in general.

References

- Alexander C, Vortuba M, Pesch UE (2000). OPA1, encoding a dynamin related GTPase, is mutated in autosomal dominant in optic atrophy linked to chromosome 3q28. *Nat Genet.* 26:211-215.
- Baxter RV, Rochelle JM (2000). GADP-1 is mutant in Charcot Marie tooth neuropathy type 2A. *Nat Genet.* 30:20-25.
- Chan DC (2006). Mitochondrial fusion and fission in mammals. *Annu Rev Cell Dev Biol.* 22:79-99.
- Chen W, Mi R, Haughey N, Oz M, Höke A (2007). immortalization and characterization of a nociceptive dorsal root ganglion sensory neuronal line. *J Peripher Nerv Syst* 12(2):121-130.
- Cho B, Choi SY, Cho HM, Kim HJ, Sun W (2013). Physiological and pathological significance of dynamin-related protein 1 (Drp1)-dependent mitochondrial fission in the nervous system. *Exp Neurobiol.* 22(3):149-157.

Clark JB, Lai JCK (1989). Glycolytic, tricarboxylic acid cycle and related enzymes in brain. In NeuroMethods, Vol. 11 (Boulton AA, Baker GB & Butterworth RF, eds.), pp. 233-281, Humana, Clifton, NJ.

De Brito OM, Scorrano L (2008). Mitofusin 2 tethers endoplasmic reticulum to mitochondria. Nature. 456:605-610.

Di Mauro S, Schon EA (2003). Mitochondria. N Engl J Med. 348:2656-2668.

Dhukande VV, Issac AO, Chatterji T, Lai JCK (2009). Reduced glutathione regenerating enzymes undergo developmental decline and sexual dimorphism in the rat cerebral cortex. Brain Res. 1286:19-24.

Dukhande VV, Kawikova I, Bothwell ALM, Lai JCK (2013). Neuroprotection against neuroblastoma cell death induced by depletion of mitochondrial glutathione. Apoptosis. 18(6): 702-712.

Fraizer AE, Kiu C, Stojanovski D, Hoogenraad NJ, Ryan MT (2007). Mitochondrial nuclear communications. Biol Chem. 387:1551-1558.

Fox TD (2004). Mitochondrial protein synthesis, import, and assembly. Nat Cell Biol. 6(11):1054–1061.

Idikuda VK (2013). Mitochondrial dynamics in Schwann cells and dorsal root ganglion neurons. M.S. Thesis, Idaho State University, Pocatello, Idaho.

Isaac AO (2007). Mitochondrial DNA depletion alters energy metabolism, antioxidant systems, and intergenomic signaling: implications in neurodegeneration, toxicity to nucleoside analogue-based HIV therapy and mitochondrial myopathies. Ph.D. Dissertation, Idaho State University, Pocatello, Idaho.

- Isaac AO, Dhukande VV, Lai JCK (2007). Metabolic and antioxidant system alterations in astrocytoma cell line challenged with mitochondrial DNA deletions. *Neurochem Res.* 11:1906-1918.
- Jaiswal AR, Bhushan A, Daniels CK, Lai JCK (2010). A cell culture model for diabetic neuropathy studies. *Journal of the Idaho Academy of Science.* 46(1):58-63.
- Kijima (2005). Mitochondrial GTPase Mfn2 mutation in Charcot-Marie Tooth neuropathy Type 2A. *Human Genet.* 116:23-27.
- King MP, Attardi G (1989). Human cells lacking mtDNA: repopulation with exogenous mitochondria by complementation. *Science.* 246:500-503.
- Kugler SK, Bahar EM (2003). Human synapsin 1 gene promoter confers highly neuron-specific long-term transgene expression from an adenoviral vector in the adult rat brain depending on the transduced area. *Gene Ther.* 10(4):337-347.
- Lai JCK, Clark JB (1989). Isolation and characterization of synaptic and non-synaptic mitochondria from mammalian brain. In *NeuroMethods*, Vol. 11 (Boulton AA, Baker GB & Butterworth RF, eds.), pp. 43-98, Humana, Clifton, NJ.
- Le Bras M, Clément MV, Pervaiz S, Brenner C (2005). Reactive oxygen species and the mitochondrial signaling pathway of cell death. *Genetics.* 20(1):205-19.
- Li Z, Srivastava P (2004). Heat shock proteins. *Curr Protoc Immunol.* 10:37-45.
- Liang LP, Patel M (2004). Iron-sulfur enzyme mediated mitochondrial superoxide toxicity in experimental Parkinson's disease. *J Neurochem.* 90:1076–1084.
- Liochev SI, Fridovich I (2007). The effects of superoxide dismutase on H₂O₂ formation. *Free Radic Biol Med.* 42(10):1465-1469.

Liu CY, Lee CF, Hong CH, Wei YH (2004). Mitochondrial DNA mutation and depletion increase the susceptibility of human cells to apoptosis. *Ann N Y Acad Sci.* 11:133-145.

Luo W, Sun W, Taldone T, Rodina A, Chiosis G (2010). Heat shock protein 90 in neurodegenerative diseases. *Mol Neurodeg.* 5:1324- 1327.

Mayer MP, Bukau B (2005). Hsp70 chaperons: Cellular functions and molecular mechanisms. *Cell Mol Life Sci.* 62(6):670-684.

Melov S (2000). Mitochondrial oxidative stress. Physiologic consequences and potential for a role in aging. *Ann N Y Acad Sci.* 908:219-225.

Pareyson D, Piscoquito G, Moroni I, Salsano E, Zeviani M (2013). Peripheral neuropathy in mitochondrial disorders. *Lancet Neurol.* 12(10):1011-1024.

Patel M, Day BJ, Crapo JD, Fridovich I, McNamara JO (1996). Requirement for superoxide in excitotoxic cell death. *Neuron.* 16:345–355.

Patergnani S, Suski JM, Agnoletto C (2011). Calcium signaling around mitochondria associated membranes (MAMs). *Cell Commun Signal.* 9:19-19.

Rigoulet M, Yoboue ED, Devin A (2011). Mitochondrial ROS generation and its regulation: mechanisms involved in H(2)O(2) signaling. *Cell Commun Signal.* 14(3):459-68.

Rosahl TW, D Spillane D, Missler M, Herz J, Selig DK, Wolff JR, Hammer RE, Malenka R (1995). Essential functions of synapsin-1 and synapsin-II in vesicle regulation. *Nature.* 375:488-493.

Rotruck JT, Pope AL, Ganther HE, Swanson AB, Hafeman DG, Hoekstra WG (1973). Selenium: Biochemical role as a component of glutathione peroxidase. *Science.* 179(4073):588-90.

- Schapira AH (1999). Mitochondrial involvement in Parkinson's disease, Huntington's disease, hereditary spastic paraplegia and Friedreich's ataxia. *Biochim Biophys Acta*. 1410:159–170.
- Taylor ER, Hurrell F, Shannon RJ, Lin TK, Hirst J, Murphy MPJ (2003). Reversible glutathionylation of complex I increases mitochondrial superoxide formation. *Biol Chem*. 278(22):19603-19610.
- Tolkovsky AM (2009). Mitophagy. *Biochim Biophys Acta*. 1793:1508-1515.
- Tretter L, Adam-Vizi V (2005). Alpha-ketoglutarate dehydrogenase: a target and generator of oxidative stress. *Philos Trans R Soc Lond B Biol Sci*. 360:2335–2345.
- Uttara B, Singh AV, Zamboni P, Mahajan RT (2009). Oxidative stress and neurodegenerative disease: A review of upstream and downstream antioxidant therapeutic options. *Curr Neuropharmacol*. 7(1):65-74.
- Vasquez-Vivar J, Kalyanaraman B, Kennedy MC (2000). Mitochondrial aconitase is a source of hydroxyl radical: An electron spin resonance investigation. *J Biol Chem*. 275:14064–14069.
- Waterham HR, Koster J (2007). A lethal effect of mitochondrial and peroxisomal fission. *N Eng J Med*. 356:1736-1741.
- Zhang L, Zhao H, Blagg BSJ, Dobrowsky RT (2012) A c-terminal heat shock protein 90 inhibitor decreases hyperglycemia-induced oxidative stress and improves mitochondrial bioenergetics in sensory neurons. *J Proteome Res*. 11(4):2581-2593.
- Zhao J, Liu T, Jin S (2011). Human MIEF1 recruits Drp1 to mitochondrial outer membranes and promotes mitochondrial fusion rather than fission. *EMBO J*. 30:2762-2778.

Ziehn MO, Avedisian AA, Dervin SM, Umeda EA, O'Dell TJ, Voskuhl RR (2012). Therapeutic testosterone administration preserves excitatory synaptic transmission in the hippocampus during autoimmune demyelinating disease. *J Neurosci.* 32(36):12312-12324.

Zorzano A (2009). Regulation of mitofusin-2 expression in skeletal muscle. *Appl Physiol Nutr Metab.* 34:433-439.

Figures and Legends

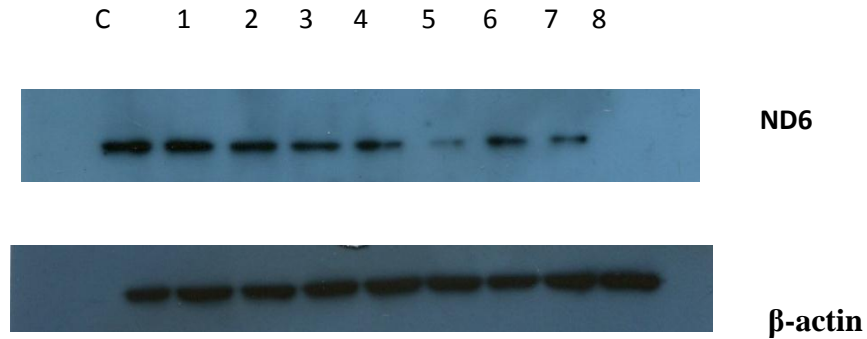


Fig. 1. Chronic exposure of DRG neurons to ethidium bromide (EB) induced time-related decreases in expression of NADH dehydrogenase subunit 6 (ND6), a polypeptide encoded by mitochondrial DNA (mtDNA), as determined by Western blot analysis.

The lane numbers, 1 to 8 represent increasing passage number of DRG neurons: the corresponding passage numbers for the EB-treated DRG neurons were 3, 7, 10, 11, 14, 16, 18, and 21, respectively; C represents control DRG neurons, not treated with EB. Equal amount (15 μ g) of protein was loaded onto each lane. The expression of β -actin served as the loading control. Note that in lane 8 expression of ND6 was not detectable. Each blot was a representative of at least three different experiments.

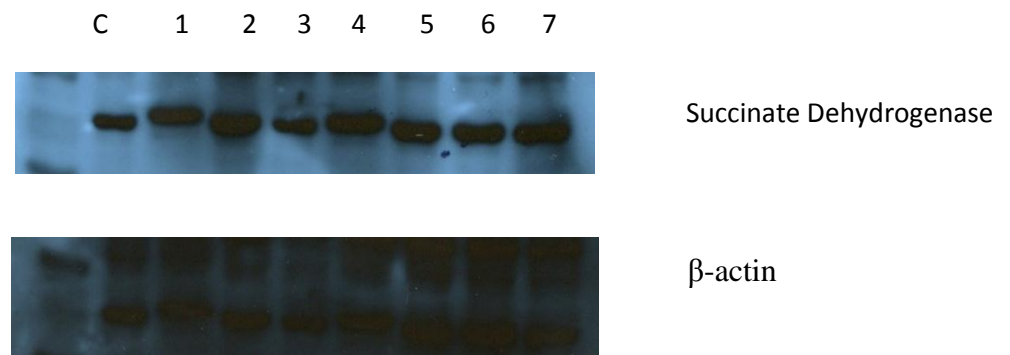
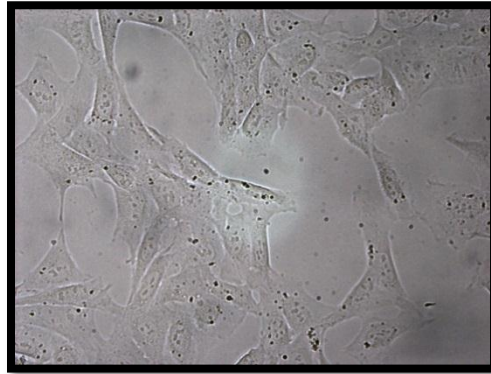
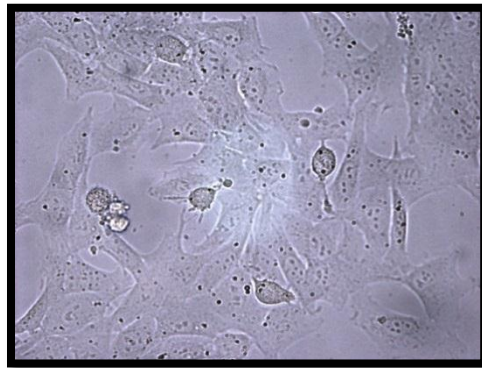


Fig. 2. Chronic exposure of DRG neurons to ethidium bromide (EB) did not induce time-related decreases in expression of succinate dehydrogenase, a polypeptide encoded by nuclear DNA, as determined by Western blot analysis.

The lane numbers, 1 to 7 represent increasing passage number of DRG neurons: the corresponding passage numbers for the EB-treated DRG neurons were 3, 7, 10, 11, 14, 16, 18, and 21, respectively; C represents control DRG neurons, not treated with EB. Equal amount (15 μ g) of protein was loaded onto each lane. The expression of β -actin served as the loading control. Each blot was a representative of at least three different experiments.



Control DRG neurons



EB-treated DRG neurons

Fig. 3. Bright field light microscopic images of the control (i.e., not ethidium bromide (EB)-treated) and EB-treated DRG neurons.

The images were acquired at 400x magnification. The images of the EB-treated DRG neurons were acquired after they had been chronically treated with EB for 14 passages. The EB-treated DRG neurons were devoid of mitochondrial DNA and appeared smaller compared to control DRG neurons.

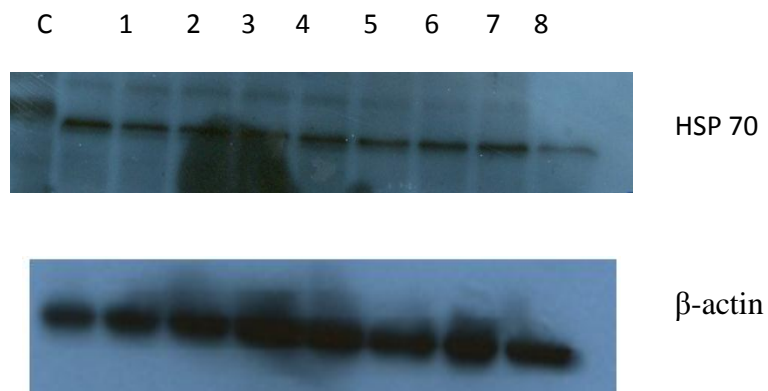


Fig. 4. Chronic exposure of DRG neurons to ethidium bromide (EB) induced time-related decreases in expression of heat shock protein 70 (HSP70), as determined by Western blot analysis.

The lane numbers, 1 to 8 represent increasing passage number of DRG neurons after treatment with EB: the corresponding passage numbers of the EB-treated DRG neurons were 15, 16, 18, 19, 20, 21, 24, and 25, respectively; C represents the control (i.e., DRG neurons not treated with EB). Equal amount (15 μ g) of protein was loaded onto each lane. The expression of β -actin served as the loading control. Each blot was a representative of at least three different experiments.

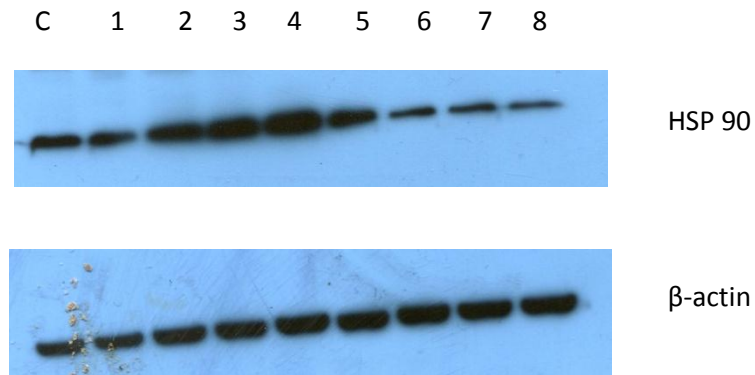


Fig. 5. Chronic exposure of DRG neurons to ethidium bromide (EB) induced time-related changes in expression of heat shock protein 90 (HSP90), as determined by Western blot analysis.

The lane numbers, 1 to 8 represent increasing passage number of DRG neurons after treatment with EB: the corresponding passage numbers of the EB-treated DRG neurons were 15, 16, 18, 19, 20, 21, 24, and 25, respectively; C represents the control (i.e., DRG neurons not treated with EB). Equal amount (15 μ g) of protein was loaded onto each lane. The expression of β -actin served as the loading control. Each blot was a representative of at least three different experiments.

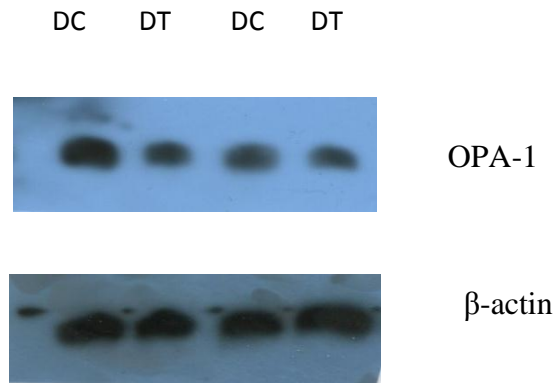


Fig. 6. Chronic treatment with ethidium bromide (EB) induced a decreased expression of optic atrophy factor-1 (OPA-1) in DRG neurons, as determined by Western blot analysis.

DT represents the EB-treated DRG neurons at passage number 19. DC represents control (i.e., DRG neurons not treated with EB). Equal amount (25 μ g) of protein was loaded onto each lane. The expression of β -actin served as the loading control. Each blot was a representative of at least three different experiments.

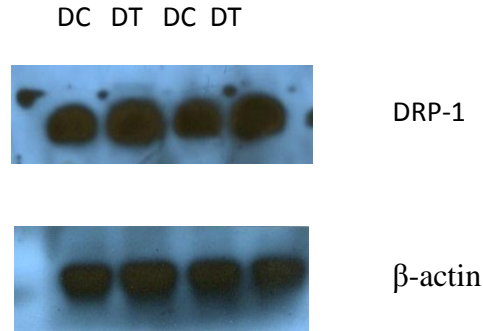


Fig. 7. Chronic treatment with ethidium bromide (EB) induced an increased expression of dynamic related protein-1 (DRP-1) in DRG neurons, as determined by Western blot analysis.

DT represents the EB-treated DRG neurons at passage number 19. DC represents control (i.e., DRG neurons not treated with EB). Equal amount (25 μ g) of protein was loaded onto each lane. The expression of β -actin served as the loading control. Each blot was a representative of at least three different experiments.

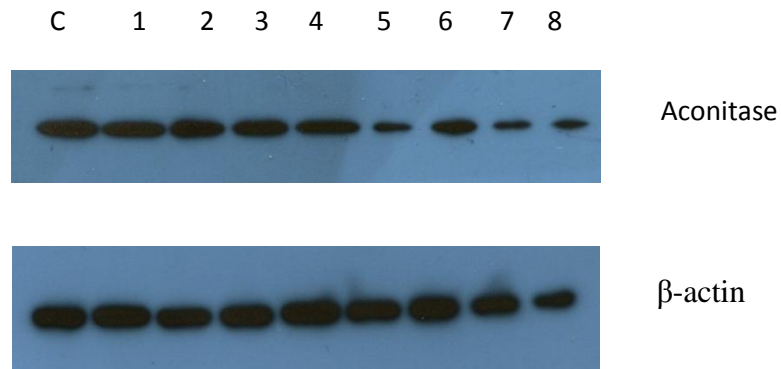
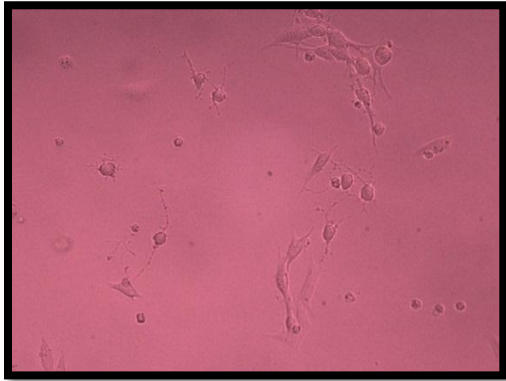
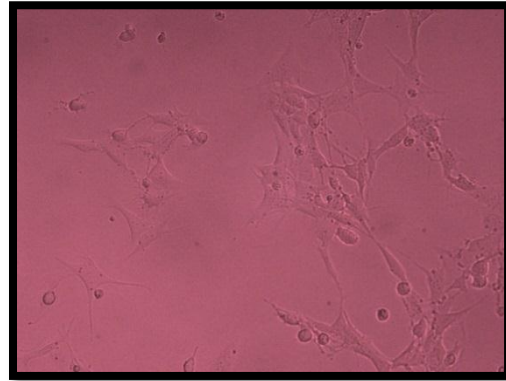


Fig. 8. Chronic exposure of DRG neurons to ethidium bromide (EB) induced time-related decreases in expression of aconitase, as determined by Western blot analysis.

The lane numbers, 1 to 8 represent increasing passage number of DRG neurons after treatment with EB: the corresponding passage numbers of the EB-treated DRG neurons were 15, 16, 18, 19, 20, 21, 24, and 25, respectively; C represents the control (i.e., DRG neurons not treated with EB). Equal amount (15 μ g) of protein was loaded onto each lane. The expression of β -actin served as the loading control. Each blot was a representative of at least three different experiments.



Control DRG neurons treated with
Forskolin



DRG neurons depleted of mtDNA
then treated with Forskolin

Fig. 9. Bright field light microscopic images of control DRG neurons treated with only 50 μ M forskolin for 48 hours (on the left) and DRG neurons depleted of mitochondrial DNA (by chronically treated with ethidium bromide for 14 passages) and then treated with 50 μ M forskolin for 48 hours (on the right).

The images were acquired at 400x magnification.

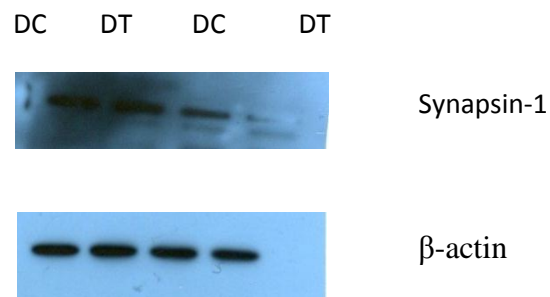


Fig. 10. Chronic treatment with ethidium bromide (EB) induced a decreased expression of synapsin-1 in DRG neurons, as determined by Western blot analysis.

DT represents the EB-treated DRG neurons at passage number 19. DC represents control (i.e., DRG neurons not treated with EB). Equal amount (15 μ g) of protein was loaded onto each lane. The expression of β -actin served as the loading control. Each blot was a representative of at least three different experiments.

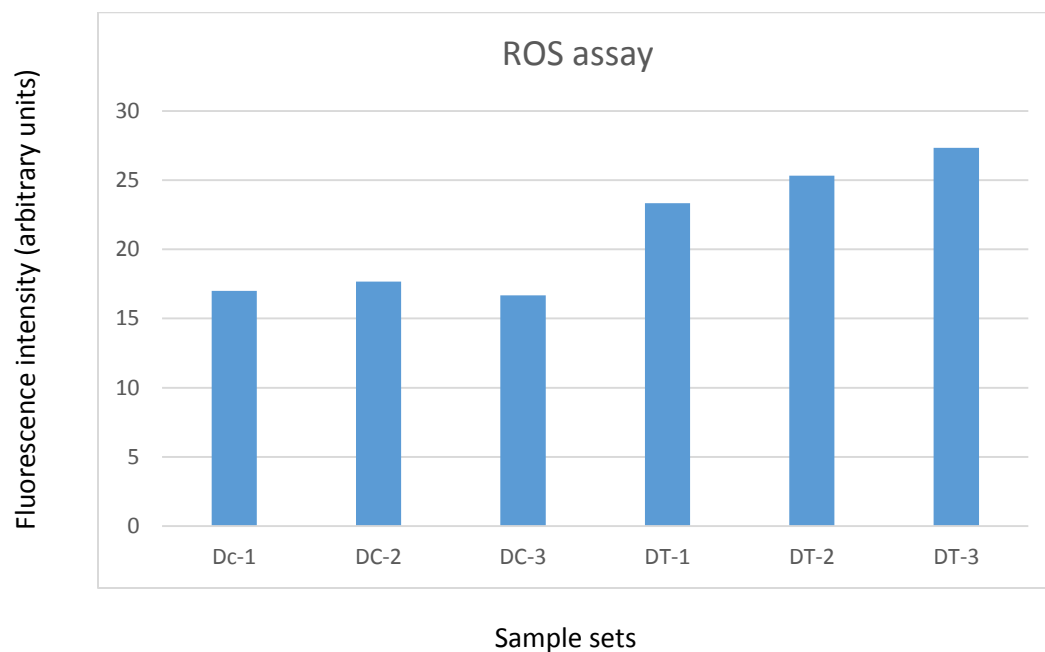


Fig. 11. Production of reactive oxygen species (ROS) by control untreated DRG neurons (DC-1, DC-2, DC-3) and by DRG neurons chronically treated with ethidium bromide (EB) to deplete their mitochondrial DNA (DT-1, DT-2, DT-3).

ROS production was assayed with the dye H2DCFDA using a microplate reader reading fluorescence output at 512 nm. EB-treated DRG neurons at passage 19 and control DRG neurons not treated with EB were employed.

GSH content in control and EB-treated DRG neurons

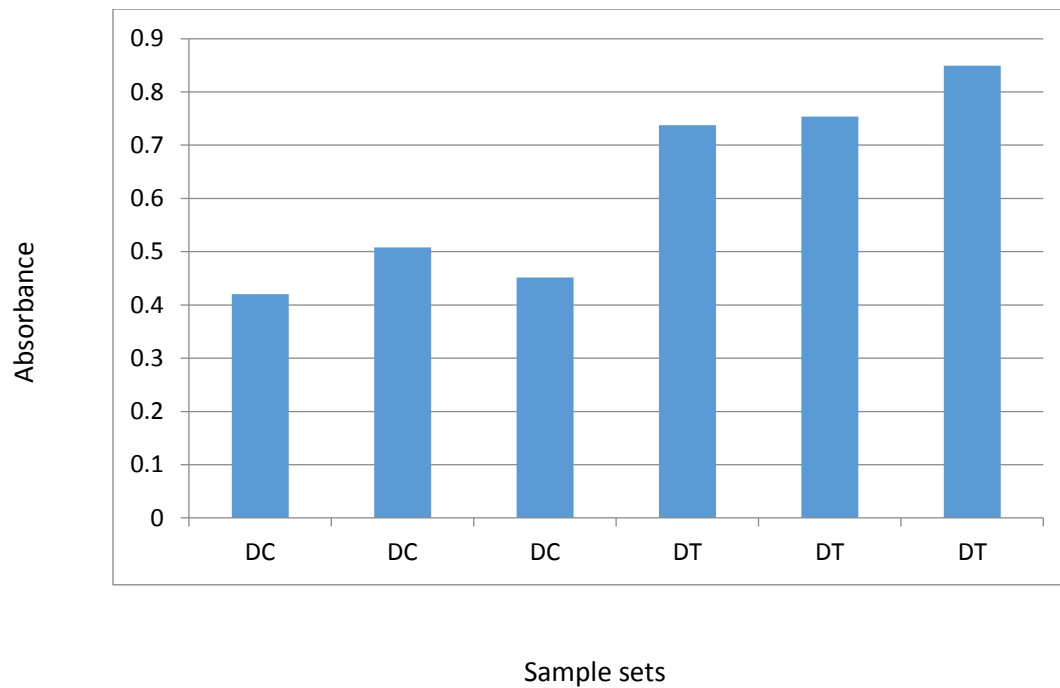


Fig. 12. Glutathione (GSH) content in control DRG neurons (i.e., not treated with EB) (DC) and DRG neurons chronically treated with ethidium bromide (EB) to deplete their mitochondrial DNA (DT).

EB-treated DRG neurons at passage 19 and control DRG neurons not treated with EB were employed.

Chapter 4

Conclusions and Prospects for Future Studies

Conclusions

To be able to investigate the effects of mtDNA depletion on peripheral neurodegeneration, we generated a DRG cell line with significant and gradual loss of mitochondrial DNA. It is important that mtDNA and nDNA signaling play an important role in diseases that exhibit ETC defects and mtDNA damage. Hence the aim of our study was to identify the role of mtDNA in cellular metabolism, antioxidant function, mitochondrial dynamics and inter-genomic communication (i.e., communication between the mitochondrial and the nuclear genomes).

Our results showed that there were alterations in metabolic and antioxidant systems, and exhibited differential effects in DRG neurons and Schwann cells that had depleted of their mtDNA. DRG neurons were more susceptible to mtDNA depletion induced by ethidium bromide compared with Schwann cells. In both the cells lines, expression of ND6 was lost prior to loss of COX2. Our results also demonstrated down regulation of aconitase, citrate synthase and malate dehydrogenase (TCA cycle enzymes) and upregulation of hexokinase and lactate dehydrogenase (glycolytic and related enzymes) in DRG neurons depleted of their mtDNA.

We have also investigated the effects of mtDNA deletion on oxidative stress and we have found DRG neurons depleted of their mtDNA exhibited an increase in their production of ROS, which can be attributed to decrease in the expression of manganese super oxide dismutase. We also found that the DRG neurons devoid of mtDNA contained higher levels of GSH compared to those in normal DRG neurons, suggesting a compensatory mechanism in DRG neurons depleted of their mtDNA to cope with increased production of ROS.

Our results also indicated mt-DNA deletion induced changes in the expression of fission and fusion proteins in DRG neurons. While there was a decrease in the expression of fusion proteins (Mfn-1, Mfn-2, OPA-1), the expression of fission protein, DRP-1 was found to be upregulated implying altered mitochondrial dynamics, a conclusion that is consistent with our morphological findings employing confocal microscopy.

To determine if mtDNA deletion induces any disruptions in intergenomic communications, we have investigated the effect of mtDNA depletion on the expression of molecular chaperones in DRG neurons. In this study, we found that chronic deletion of mtDNA induces time-related decreases in their expression of HSP70 and alterations their expression of HSP90.

We have also investigated the possibility that chronic mtDNA deletion may induce changes in synaptic plasticity and integrity in DRG neurons by examining the expression of synapsin-1 in DRG neurons devoid of mitochondrial DNA. Our finding suggests that chronic deletion in mtDNA induces decreases in synapsin-1 expression implying that depletion of mtDNA in DRG neurons induces changes in their structural and synaptic plasticity.

Our findings strongly suggest that intact mitochondrial DNA is essential for normal cellular function in DRG neurons and Schwann cells and deletion of mtDNA in DRG neurons disrupts their intergenomic communication between nDNA and mtDNA. In addition, our results also suggest mtDNA deletion induces metabolic and antioxidant system alterations in DRG neurons and these alterations can serve as markers for mitochondrial dysfunction. Moreover our results also indicate depletion of mtDNA in DRG neurons disrupts the equilibrium between

mitochondrial fission and fusion in these cells and alters their expression of heat shock proteins (especially HSP70 and HSP90) and synapsin.

More specific conclusions can be drawn from the findings of the current work. (1) mtDNA depletion alters the expression of key glycolytic and related and TCA cycle enzymes. (2) mtDNA depletion in DRG neurons alters their antioxidant system and induces an enhancement in their production of ROS. (3) Intact mtDNA is required for signaling between nDNA and mtDNA and other inter-genomic communication. (4) Depletion in mtDNA in DRG neurons increases their expression of OPA- 1 while it decreases their expression of DRP-1. (5) mtDNA depletion in DRG neurons induces decreases in their expression of synapsin-1, suggesting that mtDNA depletion induces changes in their synaptic and other morphological plasticity.

Prospects for Future Studies

The research in the field of mitochondrial dynamics is increasing as it is involved in trafficking and turnover of the mitochondria and there is a strong evidence for its role in neurodegeneration (Manczak et al., 2011). Studies have indicated changes in the mitochondrial fusion proteins, such as the mitofusins and OPA-1, leading to the peripheral nervous system disorder of Charcot Marie Tooth Disease (Chen et al., 2007). Likewise, changes in the mitochondrial dynamics and protein import have been reported in several neurodegenerative diseases such as Parkinson's disease and Alzheimer's disease (Chaturvedi et al., 2008). For instance, mitochondrial impairment caused by peroxisome proliferator-activated receptor-gamma co-activator 1 alpha (*PGC-1 α*) can shift the equilibrium between mitochondrial fission and fusion towards mitochondrial fission (Cui et al., 2006; Murphy, 2012). Our studies to date

strongly suggest that our mtDNA deletion cell models employing DRG neurons and Schwann cells are highly instrumental in facilitating the elucidation of cellular and molecular mechanisms underlying the effects of mtDNA depletion in neural cells, especially in non-tumor neural cells and their relevance to understanding pathophysiological and/or pathogenetic mechanisms in neurodegenerative diseases as well as in peripheral neuropathy. Because our studies have shown that deletion of mtDNA in DRG neurons induces changes in their mitochondrial dynamics, further studies in this area will further elucidate how these changes in mitochondrial dynamics may be pathophysiological linked to other changes in their cellular functions. For example, we could employ live cell imaging to determine such changes in mitochondrial dynamics in real time.

Because some of our results also demonstrate that mtDNA deletion induces changes in synapsin expression in DRG neurons, further studies will be productive in revealing how mtDNA deletion induces changes in their synaptic and or morphological plasticity. Clearly, this is an area that will lead to many new and mechanistically exciting avenues.

References

- Chaturvedi RK, Beal MF (2008). PPAR: a therapeutic target in Parkinson's disease. *J Neurochem.* 106:506–518.
- Chen H, McCaffery JM, Chan DC (2007). Mitochondrial fusion protects against neurodegeneration in the cerebellum. *Cell.* 130:548–556.
- Cui L, Jeong H, Borovecki F, Parkhurst CN, Tanese N, Krainc D (2006). Transcriptional repression of PGC-1 α by mutant huntington leads to mitochondrial dysfunction and neurodegeneration. *Cell.* 127:59–69.
- Manczak M, Calkins MJ, Reddy PH (2011). Impaired mitochondrial dynamics and abnormal interaction of amyloid β with mitochondrial protein Drp1 in neurons from patients with Alzheimer's disease: Implications for neuronal damage. *Hum Mol Genet.* 20:2495–2509.
- Murphy AN (2012). Elevated PGC-1 α activity sustains mitochondrial biogenesis and muscle function without extending survival in a mouse model of inherited ALS. *Cell Metab.* 15:778–786.